Biotic and Abiotic Carbonate Records of Paleocean Chemistry: Muleshoe Mound, Mississippian Lake Valley Formation, Alamogordo, New Mexico

Franciszek Józef Hasiuk

Department of Geological Sciences
University of Michigan – Ann Arbor

December 2005


THE UNIVERSITY OF MICHIGAN
LIBRARIES
THE UNIVERSITY OF MICHIGAN
ARTES SCIENTIA VERITAS
1817

Author

Franciszek Józef Hasiuk

Title

Biotic and Abiotic Carbonate Records of Paleocean Chemistry: Muleshoe Mound, Mississippian Lake Valley Formation, Alamogordo, New Mexico

submitted in partial fulfillment
of the requirements for the degree of
Master of Science in Geology
Department of Geological Sciences
The University of Michigan

Accepted by:

Signature	Dr. Kyger C Lohmann Name	12-12-05 Date
Signature	Dr. Bruce H. Wilkinson Name	12-13-05 Date
Department Chair	Dr. Joel D. Blum Name	12-13-05 Date

I hereby grant the University of Michigan, its heirs and assigns, the non-exclusive right to reproduce and distribute single copies of my thesis, in whole or in part, in any format. I represent and warrant to the University of Michigan that the thesis is an original work, does not infringe or violate any rights of others, and that I make these grants as the sole owner of the rights to my thesis. I understand that I will not receive royalties for any reproduction of this thesis.

☒ Permission granted.

☐ Permission granted to copy after: _____
Date

☐ Permission declined.

Franciszek Hasiuk
Author Signature

Biotic and Abiotic Carbonate Records of Paleocean Chemistry: Muleshoe Mound, Mississippian Lake Valley Formation, Alamogordo, New Mexico

Franciszek Józef Hasiuk

Department of Geological Sciences
University of Michigan – Ann Arbor

December 2005

Abstract

It has been proposed that oceanic Mg/Ca chemistry has varied during the Phanerozoic and has controlled primary carbonate mineralogies between aragonite-dominated and calcite-dominated "seas". A study was undertaken to assess Mississippian oceanic Mg/Ca and Sr/Ca. Marine carbonate cements offer a unique opportunity for investigating this proposition, as they are abiotic precipitates from seawater whose composition is controlled by the fluid from which they precipitate.

The Early Mississippian (Tournaisian/Visean) Muleshoe Mound (Lake Valley Fm, Alamogordo, NM) contains a diverse fauna in addition to micrite and a wide array of carbonate cements (e.g. crinoid syntaxial cements, radiaxial fibrous marine cements). Stable isotope ($\delta^{18}O$, $\delta^{13}C$) and elemental analyses as well as cathodoluminescence characteristics elucidated the diagenetic history of the bioherm and serve to identify the least diagenetically altered specimens for elemental analyses. Isotopic analyses define two diagenetic trends, both starting at values similar to inferred Mississippian marine calcite (–1.5‰ $\delta^{18}O_{VPDB}$, +4.5‰ $\delta^{13}C_{VPDB}$). A burial diagenetic trend follows from this point to lighter oxygen values (–6‰ $\delta^{18}O_{VPDB}$, +4‰ $\delta^{13}C_{VPDB}$) and a meteoric diagenetic trend can be defined with a meteoric calcite line at ~ –3‰ $\delta^{18}O$. Average elemental data for least altered phases are: Mg/Ca = 6-19 mmol/mol; Sr/Ca = 0.15-0.2 mmol/mol; Mn/Ca and Fe/Ca < 1 mmol/mol. Similarity of non-luminescent cement and non-luminescent crinoid data suggest that crinoid material has been completely replaced by cement.

Using a generally accepted $D_{Mg}^{calcite}$ of 0.015 to 0.02, the Mg/Ca for Mississippian seawater ranged from 0.3 to 0.9 mol/mol, in comparison to the modern value of 5.1. Mg/Ca in this range is compatible with the Early Mississippian being a time of "calcite seas", and compares well with the Devonian value (0.49) of Carpenter et al. (1991). It is somewhat lower than the Phanerozoic Mg/Ca minimum of 1.0 mol/mol suggested by geochemical modeling (Hardie, 1996).

Using a range of $D_{Sr}^{calcite}$ of 0.22 to 0.33 and the average Sr/Ca from the unaltered phases, the Sr/Ca for Mississippian seawater averages between 0.3 and 0.9 (mmol/mol), in comparison to the

modern value of 8.8.

Introduction

The oceans mediate all biogeochemical cycles, regulate global climate, and comprise the largest ecosystem on Earth. Just as the study of modern ocean chemistry has provided valuable insight into the nature of modern Earth systems (e.g. thermohaline circulation), a robust geological perspective on ocean chemistry elucidates not only the possible ranges of seawater composition, but also clarifies the nature of the processes responsible for those changes (inevitably, the eternal drumbeat of plate tectonics) and their temporal variability. There is no greater insight into Phanerozoic marine chemistry than that afforded by the subtle variation in mineralogy and geochemistry of marine carbonate. Much more abundant than evaporites, carbonates are the second most common chemical sedimentary rock, accounting for some 20% of the sedimentary rock record.

The dominant polymorph of calcium carbonate has been suggested to vary through geologic time in relation to ocean chemistry (Sandberg, 1983; Hardie, 1996; Lowenstein et al., 2001). While metastable aragonite and high-Mg calcite cements and skeletal debris dominate the mineralogy of Holocene tropical shallow-water carbonates, numerous studies (e.g. Sandberg, 1975) document ancient carbonates composed of original calcite recognized by the preservation of primary microfabrics. The factors controlling this Phanerozoic-scale alternation in primary carbonate mineralogy remain the elusive focus of numerous inquiries by sedimentary geologists and chemical oceanographers working to unravel the geologic history of seawater.

Previous Work

In a pioneering petrographic study, Sandberg (1975) recognized variation of crystalline fabric preservation in ooliths. Fabric preservation varied from fine retention of primary concentric and radial structures in some specimens to the complete lack of discernible fabrics in others. On this basis, Sandberg (1975) concluded that those preserving crystalline microfabrics

were precipitated as calcite, whereas those lacking discernible fabrics represented a primary mineralogy of aragonite that had diagenetically stabilized to calcite. Incorporating the work of Mackenzie and Pigott (1981), Sandberg (1983) provided a more comprehensive synthesis based on the "greenhouse/icehouse" cycles of Fischer (1981) suggesting that the primary mineralogy of Phanerozoic marine carbonate has oscillated between what he termed "calcite seas", when low-Mg calcite precipitation was strongly favored over aragonite and high-Mg calcite production, and "aragonite seas", when conditions were more favorable for aragonite and high-Mg calcite production alongside, and still likely subordinate to, calcite production (Figure 1B). Although this secular trend in carbonate mineralogy has been documented by others (e.g. Stanley and Hardie, 1998; Lowenstein et al., 2001), the physico-chemical factors controlling it remain poorly understood.

Based on previous work (Lippman, 1960; Folk, 1974), Sandberg (1975) suggested that the ratio of Mg^{2+} to Ca^{2+} ions in the fluid from which the precipitation occurs is the principal control on this mineralogical variation either by means of surface poisoning (Folk, 1974; Berner, 1975), thermodynamic destabilization (Davis et al., 2000), or a combination of the two (Gutjar et al., 1996).

Hardie (1996) reported a similar trend in evaporite mineralogies, which was theorized to be arbitrated by oceanic Mg/Ca. Mg-SO_4 salts predominated during "aragonite seas" due to higher Mg/Ca and K-Cl salts during "calcite seas" due to the lower Mg/Ca. However, the apparent decrease in oceanic Mg content could be driven by changes in dolomite formation. Comparing Hardie's trends to the Phanerozoic dolomite abundance curve of Given and Wilkinson (1987), it can be discerned that dolomite is abundant during Hardie's "K-Cl seas" and scarce during "Mg-SO_4" seas. Perhaps the formation of dolomite is acting as a sink for Mg that would have lead to the formation of Mg-SO_4 evaporites. Kovalevich et al. (1998), summarizing the relevant extant Russian literature, generated a more complex time series of Phanerozoic evaporite mineralogy (Figure 1C).

Empirical values of Phanerozoic seawater chemistry have been pursued using a variety

of approaches. A voluminous literature derives from studies of evaporite fluid inclusions (e.g. Kovalevich et al. 1998, Lowenstein et al. 2001, Horita et al. 2002). And despite the equally numerous factors that must be accounted for when using this method (e.g. brine evolution, hydrologic conditions) it remains quite appealing to directly analyze the chemistry of relict fluids from various points in geologic time. Biotic carbonate phases offer another tantalizing glimpse into the evolution of ocean waters since they are both abundant and easily datable within the geologic record. Stanley and Hardie (1998) suggest that aragonite secreting organisms thrive during "aragonite seas" and calcite producers during "calcite seas". Separately, echinoderms have been suggested both to change their skeletal Mg content in relation to changing seawater chemistry (Ries, 2004) and to remain fixed in composition through time (Dickson, 2004). This is a good example of how vital effects can obscure such secular changes in biotic phase composition (Weber and Raup, 1966).

Inorganic carbonate precipitates offer another opportunity to decipher paleo-seawater chemistry, by avoiding the ambiguities related to unresolved vital effects or the difficult to quantify pathways of brine evolution. Whether precipitated within porosity (marine cements) or as coatings (ooliths, pisoliths, etc), they display distinct geochemistries based on the physical and chemical characteristics of their depositional environment. The challenge of using the cement record is to constrain the diagenetic history, which the material has undergone. A multi-faceted approach of petrography and geochemical analysis of the component phases is the key to establishing the fidelity of any cement record (e.g. Carpenter et al., 1991).

It is the goal of this study to test the hypothesis that a "calcite sea" existed during times of low oceanic Mg/Ca by examining geochemical proxies in abiotic marine cements and co-occurring crinoids at Muleshoe Mound. The depositional environment and the subsequent thermotectonic history of the bioherm are well known and a plethora of work has been completed on the diagenetic history of the cement phases occluding primary porosity. Within this context, one can refine our understanding of the chemical characteristics of Mississippian seawater, compare it to previous estimates for the Mississippian, and evaluate whether these characteristics

support the proposed tenets of "calcite/aragonite seas".

Methods

Location, stratigraphic context, and paleogeography

Numerous Waulsortian-type mud mounds, ranging in height from 5 to 100 meters, are well exposed in the strata of the Lower Carboniferous (Mississippian) Lake Valley Formation, outcropping on the western escarpment of the Sacramento Mountains, near Alamogordo, New Mexico (Figure 2). Muleshoe Mound, one of the largest bioherms in the Sacramento Mountains at 100 m thick, outcrops approximately 6 km south of Alamogordo. Muleshoe Mound developed on a homoclinal ramp dipping to the south at a low latitude (Ahr, 1989). The morphology of Muleshoe is typical of a carbonate mud mound whose growth was truncated by storm wave base with concomitant development of off-mound debris deposits (Schlager, 2003). Accretion occurred near or below the photic zone (Ahr and Stanton, 1996). Muleshoe Mound is truncated at an unconformable contact with overlying Upper Carboniferous (Pennsylvanian) units. Kirkby and Hunt (1996) delineated five phases of mound growth, beginning in with Alamogordo Member (Figure 3) mound initiation, fostered by swift currents and well oxygenated waters. Each phase of growth was punctuated by mound crises when stagnant, poorly oxygenated waters asphyxiated mound biota.

Sampling regime

Samples were collected from as broad a stratigraphic and geographic range on the mound as the local topography and vegetation would allow. The major facies and depositional features from which samples were taken include: the fenestrate bryozoan cementstone core, the crinoidal grainstone flank units, and the Neptunian dikes crosscutting the bioherm. Where the massive nature of the bioherm prevented easy collection of handsamples, a water-cooled "paleomag" drill was used to obtain 10-15 cm cores.

Phases analyzed

Optical petrography of 78 thinsections established the distribution and character of allochems, micrite, and cements in collected samples. Three lithologies dominate the specimens. The accretionary core of Muleshoe Mound is characterized by a bryozoan cementstone, which contains abundant fenestrate bryozoan debris, abundant fibrous to blocky cement, common crinoid columnals, minor ostracod debris, micrite and other fossil debris. Off-mound flank beds are dominantly crinoidal debris encased in syntaxial cements. Neptunian dikes crosscutting the mound are mostly composed of micrite, which contain scattered, common to rare, crinoidal fragments.

Cathodoluminescence petrography qualitatively established the degree of alteration of the various constituents with non-luminescent phases supposed relatively unaltered, and luminescent phases relatively altered. Non-luminescent fibrous cements from the bryozoan cementstone were analyzed as representing syndepositional marine cement. In addition, luminescent, variably and alternatingly luminescent, and non-luminescent crinoids were selected for geochemical analysis from all three main lithologies. These five phases (Figure 4) account for 150 of 175 paired isotopic and elemental analyses. The remainder of the analyses were carried out on luminescent fibrous cements, speleothem cements, bryozoans, brachiopods, and micrite (Appendix 1, Appendix 2).

Syntaxial cements and blocky calcite spars were generally avoided as previous work (Meyers, 1974; Meyers and Lohmann, 1985) had shown them to predominantly originate during meteoric and/or burial diagenesis.

Analytical methods

Bulk sampling was performed using a dental drill to manually extract ~100 μg-sized powders from 0.5 mm^2 areas of crinoids, micrites, and speleothem cements. A Merchantek (New Wave) MicroMill computer-controlled drilling system was used to recover ~50 μg-sized powders from petrographic thinsections of cements, crinoids, and other fossil materials that were chosen based

on luminescent character. Resultant powders were split for paired stable isotopic and elemental analysis.

Splits for isotopic analysis were roasted *in vacuo* for one hour at 200°C to remove volatile contaminants and water. They were then reacted with anhydrous H_3PO_4 at 76 ± 2°C in a Kiel automated carbonate preparation device coupled directly to the inlet of a Finnigan MAT mass spectrometer at the University of Michigan's Stable Isotope Laboratory. ^{17}O-corrected data are adjusted for acid fractionation and source mixing by calibration to a best-fit regression line defined by NBS-18 and NBS-19 standards. Data are reported in ‰-variation relative to the V-PDB standard. Measured precision is better than 0.1‰ for both $\delta^{13}C$ and $\delta^{18}O$.

Splits for elemental analysis were dissolved with 1 ml 0.1N HNO_3. 1.6 ml of 0.1N HNO_3 was added to 0.4 ml of the dissolved split for analysis via Finnigan Element ICP-MS at the University of Michigan's Keck Environmental Geochemistry Laboratory. Samples were calibrated to run at a constant Ca concentration to correct for matrix effects. ^{24}Mg, ^{42}Ca, ^{43}Ca, ^{44}Ca, ^{88}Sr were analyzed at low resolution. ^{44}Ca, ^{55}Mn, and ^{57}Fe were analyzed at medium resolution. Machine data (in parts-per-thousand) was then converted to atom fractions.

Results

Two distinct diagenetic trends can be discerned from a cross plot of carbon and oxygen isotope values (Figure 5A), similar to that reported by Cicero and Lohmann (2001) for Silurian cements from Indiana.

A meteoric diagenetic trend is defined by analyses with highly variable $\delta^{13}C$ and comparatively invariable $\delta^{18}O$ (a meteoric calcite line *sensu* Lohmann, 1988) at ~ –3‰. Analyses intermediate on this trend have the highest Mn/Ca ratios of all samples analyzed and samples with the most negative $\delta^{13}C$ show elemental ratios near zero indicating precipitation from meteoric waters.

A burial diagenetic trend of increasingly more negative $\delta^{18}O$ and slightly more negative $\delta^{13}C$

is also discernable in CO-space (Choquette and James, 1990). The burial diagenetic trend ranges from –1‰ and -6.5‰ $\delta^{18}O$ and 4.5‰ and 6‰ $\delta^{13}C$ with scatter of about 1‰ $\delta^{13}C$ at any given $\delta^{18}O$. Marine cement Mg/Ca remains relatively constant with more negative $\delta^{18}O$, while crinoid Mg/Ca increases (Figure 6A). Sr/Ca demonstrates negligible change with more negative $\delta^{18}O$ (Figure 6B). Analyses along this trend also displayed the increasing Fe/Ca ratios indicative of burial diagenesis (Figure 6C). Mn/Ca values peak at ~ –3% $\delta^{18}O$, the location of the meteoric calcite line (Figure 6D).

Crinoid skeletal material displaying alternating luminescent/non-luminescent banding (herein referred to as "tiger" crinoids) had no distinct geochemical signature other than that some of the class, which fell near the end of burial diagenetic trend in CO-space, yielded the highest Mg/Ca of all phases (Figure 6A).

Since both trends converge at an isotopic composition similar to published estimates of Mississippian carbonate (Appendix 3), we assume that phases with the most positive $\delta^{18}O$ have undergone the least amount of diagenetic alteration since their $\delta^{18}O$ is most similar to the inferred Mississippian marine calcite. Based on models of rock-water diagenetic interaction, it has been shown that when original marine cement $\delta^{18}O$ values are preserved, the elemental chemistries of the original marine cement must also be preserved. For example, Cicero and Lohmann (2001) argue from rock-water reaction modeling that as long as the rock:water ratio is greater than 1%, elemental chemistries should be preserved.

Geographic Patterns

Since sample locations were recorded with accuracy of ±5m via GPS, geographical distributions of stable isotope and elemental analyses can be easily plotted. This greatly eases data interpretation when samples have been collected on a large three-dimensional object like a bioherm. $\delta^{18}O$ values show their widest range (upwards of 5‰) at the center of the mound, while those samples analyzed from its periphery show much smaller ranges (~2‰). The most negative $\delta^{18}O$ values also appear in this central area. $\delta^{13}C$ values are relatively constant across the mound,

but average slightly more negative for sites from the southeast part of the mound. Mg/Ca, Sr/Ca, and Fe/Ca have their highest values and highest ranges in the central area of the mound that also displayed the highest $\delta^{18}O$ ranges. Mn/Ca shows no trend when plotted against sample location.

Fidelity of the Muleshoe Record

Muleshoe vs. Modern isotopic data

Insight gleaned from Muleshoe data must be viewed through the prism of modern analogs. The stable isotope datasets of Weber and Raup (1965) and Weber (1968) on modern echinoderms and of Gonzalez and Lohmann (1985) and Carpenter and Lohmann (1992) on modern marine cements (Figure 5B) display wide variation a distinct trend: modern echinoderms display more negative $\delta^{13}C$ than modern marine cements. To Weber and Raup (1966), this relation indicates that echinoderms exert considerable control over the carbon isotopic compositions of their skeletal material. This was ascribed to efficiency with which crinoids we able to expel respiratory CO_2 from their visceral fluids. For example, the isotopic compositions of ophiuroids tests are the closest to inorganic carbonate values because they expel metabolic CO_2 faster than the other orders. Crinoids, on average a –10‰ offset from marine cements, have very low efficiency since their small visceral mass lacks a robust respiratory system (Weber, 1968).

Temperature, and by proxy depth, is suggested to be the first order control on oxygen isotope composition, but a weak vital effect has also been reported (Weber and Raup, 1968). The range in $\delta^{18}O$ range for each class is approximately 6‰ (Figure 5B), but echinoids and ophiuroids span from +2 to –4‰ and crinoids and asteroids span from 0 to –6‰.

In comparison, Muleshoe crinoids display isotopic compositions similar to co-occurring marine cements. Crinoid data do not overlap with the modern crinoid Carbon-Oxygen-field (Figure 5A). This suggests that some post-mortem alteration of the skeletal material has occurred, unless we wish to suggest that modern crinoids have evolved less efficient means of expelling respiratory CO_2 in the last 350 My. If anything, modern crinoids should be more efficient since the average size of crinoid coelomic cavities has decreased since the Mesozoic/

Paleozoic (T. Baumiller, pers. comm.). A high-CO_2, and thus low pH, internal cavity would be exactly the opposite of what is beneficial to an organism, which produces a large amount of carbonate skeletal material in relation to its visceral mass. Modern echinoderms can have anywhere between 63 and 91 weight % skeletal material (Emson, 1984), with crinoids at 85%.

Muleshoe vs. Modern elemental data

To compare the Muleshoe elemental data to a modern baseline, we must first evaluate the Muleshoe dataset to identify samples whose elemental or isotopic signatures suggest diagenetic alteration. Samples were disqualified under the following criteria: Mn/Ca > 1 mmol/mol, which correlates strongly with luminescent meteoric phases; $\delta^{13}C < 3‰$, which correlates with meteoric phases; Fe/Ca > 1 mmol/mol, Mg/Ca > 20 mmol/mol, $\delta^{18}O < -3.7‰$, which are characteristic of burial phases and thus don't reflect precipitation from seawater.

The data passing these tests can be interpreted as reflecting analyses of least-altered phases (Figure 7A). On a cross plot of Sr/Ca vs. Mg/Ca (Figure 8), these least-altered Muleshoe crinoid and cement data overlap, whereas modern data do not. While the slope of Mississippian brachiopod data:

$$\left(\frac{Sr}{Ca}\right)_{Brachiopod} = 0.033\left(\frac{Mg}{Ca}\right)_{Muleshoe} + 0.5351,\ r^2 = 0.68$$

differs by a factor of approximately two from the slope of the Muleshoe data:

$$\left(\frac{Sr}{Ca}\right)_{Brachiopod} = 0.014\left(\frac{Mg}{Ca}\right)_{Muleshoe} + 0.0306,\ r^2 = 0.71$$

It does suggest that some offset between biotic and abiotic phases did exist in the Mississippian.

Mucci and Morse (1990) suggest that Sr incorporation in calcite is directly proportional to Mg incorporation. Beginning again with modern data, biotic and abiotic calcite phases define distinct zones in Sr-Mg space (Figure 7B). Sr and Mg in modern echinoderms (Thompson and Chow 1955, Weber 1969, Carpenter and Lohmann 1992) and marine cements (Carpenter and Lohmann 1992) covary along trends with similar slopes, but different y-intercepts. Carpenter et al. (1991) attribute this as a "kinetic" offset in Sr incorporation caused by faster precipitating

biotic phases, though recent brachiopod data of Brand et al. (2003) cast some doubt on the simplicity of this correlation.

Several hypotheses could explain these isotopic and elemental patterns. Analyses could reflect the filling of the crinoid's stereom with a secondary low-Mg calcite. Modern echinoderms produce a highly porous skeletal material possessing a geometric feature known as a periodic minimal surface, most eloquently described by DuBois (1990) as a surface "dividing space into two interpenetrating regions, each…a single, multiply connected domain with no connection to the other". The modern echinoderm skeletal material is a magnesian calcite with 100 to 200 mmol/mol Mg/Ca and porosities ranging between 11 to 52% (Weber, 1969). To achieve our average of 10 mmol/mol Mg/Ca, even the least magnesian modern crinoids (ca. 100 mmol/mol Mg/Ca) would require 90% porosity filled with a low-Mg cement.

Uniformitarianism dictates that we consider the present the key to the past, so our null hypothesis must be that biomineralization in ancient skeletal carbonate producers proceeded in ways similar to modern relatives and that Mississippian marine cements precipitated similarly to modern marine cements. This hypothesis would lead us to believe that the Muleshoe crinoids have been completely altered in response to synsedimentary diagenesis.

Evolutionary change in the subsequent 350 My could have changed the way in which organisms biomineralized. But why would this change in vital effect have occurred and how could it be constrained if it had? Also, these patterns could be said to reflect the diagenetic alteration of both the cements and the crinoids. However, both categories of material display isotopic signatures equivalent to what has been estimated for Mississippian marine calcite. A final alternative may be that Muleshoe could have been a unique marine microenvironment, where accurate proxies of open marine seawater chemistry were not recorded, but crinoids require normal marine seawater to function with very low turbidity.

The failure to disprove the null hypothesis suggests that crinoids living on Muleshoe Mound in the Mississippian displayed similar elemental and isotopic trends as modern crinoids and

that complete replacement of their skeletal material occurred in marine fluids, erasing their original geochemical signature. MacQueen et al. (1974) reported a similar relationship between recent and Pleistocene specimens of the same species of echinoid from Shark Bay, Australia. Recent examples from Shark Bay averaged 150 mmol/mol Mg/Ca. Of the Pleistocene examples collected, three-quarters averaged 40 mmol/mol Mg/Ca and the remaining quarter ranged from 41 to 200 mmol/mol.

In fact, 24 of 35 non-luminescent cements failed one of our alteration tests, while only 6 out of 34 non-luminescent crinoids failed. This suggests that non-luminescent Muleshoe crinoid debris is really a *cement in crinoid's clothing*, preserving the same chemistry as co-occurring marine cements but with greater fidelity. This reduction in diagenetic susceptibility could result from the unit-crystal substrate, on which the crinoid was replaced with low-Mg calcite cement, possessing a much smaller surface area-to-volume ratio compared to fibrous marine cements.

Estimating Mississippian Seawater Chemistry

Several previous studies of the Lake Valley Formation determined Mg-contents of its various carbonate constituents. Point counts of microdolomite abundance in syntaxial cements by Meyers and Lohmann (1978) resulted in Mg/Ca ratios between 50 and 100 mmol/mol. Leutloff and Meyers (1984) performed a regional reconnaissance of Lake Valley echinoderm Mg contents around southwest New Mexico. From point counts of microdolomite abundance, they obtained between 100 and 150 mmol/mol Mg/Ca. The last two studies, which reported high-Mg contents for crinoids, neither generated their data through direct geochemical analysis nor were able to constrain the extent of diagenetic alteration of the samples used in their analysis; thus, their results must be viewed cautiously. Via electron microprobe, Lohmann and Meyers (1977) found microdolomite inclusions distributed in former marine cement and crinoid skeletal material, the calcite and microdolomite together average 18 mmol/mol Mg/Ca. MacQueen and Ghent (1970) analyzed Mississippian (Osagean and Meramecian) echinoderms from localities in Alberta, Canada, via electron microprobe and reported average Mg, Ca, and Fe contents. Fe in all cases

was below 0.32 mmol/mol Fe/Ca. Echinoderm Mg contents averaged 13 mmol/mol Mg/Ca similar to the analyses reported here for Mulsehoe cements and crinoids (10 mmol/mol). Douthit (1990) reported marine cements with 9 mmol/mol Mg/Ca from time and environment-equivalent Irish Waulsortian mounds. Similar signals from widely different locations suggest a similar fluid composition for the precipitation of all three cements.

The Distribution Coefficient

In order to quantify the reaction process whereby an elemental impurity is adsorbed onto the surface of a crystallizing solid and then incorporated within it, it is customary to use a distribution coefficient, D_{Me}. Distribution coefficients define the relationship between minor (or trace) element concentrations between solution and precipitate:

$$D_{MinorElement}\left(\frac{MinorElement}{MajorElement}\right)_{Solution} = \left(\frac{MinorElement}{MajorElement}\right)_{Precipitate}$$

The estimation of these coefficients dates back to the early 20th century (e.g. Doerner and Hoskins, 1925). Recent syntheses of empirically and theoretically determined distribution (or partition) coefficients have been produced by Rimstidt et al. (1998) and Curti (1999).

In addition to an equilibrium partitioning process, precipitation rate also has been shown to affect distribution coefficients due to its relation to temperature and surface area (Mucci and Morse, 1983). With faster rates (from higher temperatures and larger surface areas) promoting distribution coefficients approach unity, whereas slower rates are more likely to more result in equilibrium distribution coefficients. Crinoid skeletal material precipitates more quickly (months to years) than marine cements (years to hundreds of years) and thus the distribution coefficients for cation incorporation should be higher for crinoidal skeletal carbonate.

For the calcites of this study, we are most concerned with the incorporation of Mg and Sr, since they along with Ca are the most abundant divalent ions in the ocean. Due to ionic radius, and to a lesser extent electronegativity, Mg fits more easily into the calcite crystal structure than does Sr. However, the incorporation of Mg, somewhat smaller than Ca, is suggested to enhance the incorporation of Sr, which is somewhat larger (Mucci and Morse, 1983).

Distribution coefficients for Mg range from 0.01 to 0.12. Fuchtbauer and Hardie (1976) obtained a value of 0.031. Calculating a $D_{Mg}^{Calcite}$ from modern crinoids using seawater Mg/Ca (5.1 mol/mol) and Weber's average crinoid Mg composition (140 mmol/mol), we obtain a $D_{Mg}^{Calcite}$ of 0.027. Holocene marine cements have on average 174 mmol/mol Mg/Ca leading to a $D_{Mg}^{Calcite}$ of 0.034 (Carpenter and Lohmann, 1992). Mucci and Morse (1983) obtained values between 0.015 and 0.02 for $D_{Mg}^{Calcite}$ from inorganic carbonate precipitation experiments conducted in seawater, and thus seem the most reasonable for this investigation.

Distribution coefficients for Sr in calcite range from 0.02 to 0.33. Using a modern oceanic Sr/Ca = 8.7 mmol/mol, a $D_{Sr}^{Calcite}$ of 0.15 can be calculated from modern marine cement Sr contents. Average echinoderm Sr/Ca is 2.7 mmol/mol (Thompson and Chow, 1955) resulting in a $D_{Sr}^{Calcite} = 0.3$. Tesoriero and Pankow (1996) reported $D_{Sr}^{Calcite}$ of approximately 0.021 though their experiments were carried out in the absence of Mg, at a pH = 6, and at $pCO_2 = 0.1$ atm. Carpenter and Lohmann (1992) reported Holocene marine cements with an average of 1.72 mmol/mol Sr/Ca. The most reasonable coefficients for the purpose of this study come from Mucci and Morse (1983). Abiotic calcite was precipitated from natural seawater and $D_{Sr}^{Calcite}$ values ranging from 0.22 to 0.33 were obtained.

The least altered material analyzed in this study has approximately 6 to 19 mmol/mol Mg/Ca and 0.15 to 0.2 mmol/mol Sr/Ca. From these values we can apply the above most appropriate ranges in distribution coefficients to estimate ranges for oceanic Mg/Ca and Sr/Ca for the Mississippian. For Mg/Ca, $D_{Mg}^{Calcite} = 0.015$ to 0.02 yields $Mg/Ca_{seawater}$ of 0.3 to 0.9 mol/mol. For Sr/Ca, a $D_{Sr}^{Calcite}$ of 0.22 to 0.33 yields $Sr/Ca_{seawater}$ of 0.3 to 0.9 mmol/mol.

Mg/Ca of Muleshoe crinoids

The empirical work of Ries (2004) indicates that echinoderm skeletal Mg content covaries with the Mg-content of the seawater in which it lives. This relationship, quantified by the equation:

$$\left(\frac{Mg}{Ca}\right)_{Calcite} = 0.0471\left(\frac{Mg}{Ca}\right)_{Seawater}^{0.668}$$

allows us to estimate the original composition of Muleshoe crinoids. With an average Mississippian oceanic Mg/Ca of 0.3 to 1.27 mol/mol, crinoid skeletal material would have formed with a Mg/Ca ratio of 25 mmol/mol. This value is one quarter of the lowest values reported by Weber and Raup (1966) for modern crinoids.

There are two caveats however when using this approach:(1) Ries' equation was derived from modern echinoid plates, while this study reports results from fossil crinoid columnals. Isotopically, these two orders display different compositions (Figure 5A). Furthermore, echinoids often display widely varying elemental chemistries depending on which skeletal component is analyzed (Weber and Raup, 1966). In light of these considerations, it is plausible that echinoids and crinoids have different minor element incorporation pathways. (2) The behavior of Ries' equation was not calibrated below a fluid Mg/Ca of 1 mol/mol, a value below which our theorized Mississippian ocean lies. Mg incorporation in echinoderms in fluids below Mg/Ca=1 mol/mol could display behavior not fitting Ries' equation.

The Oceanic Cation Budget

The oceanic Mg budget is the summation of a number of fluxes, but is dominated by riverine input, cation exchange at mid-ocean ridges, and the formation of Mg-rich carbonate minerals (mostly dolomite). The combination of these fluxes results in an oceanic Mg residence time of ~10 My.

Mottl and Wheat (1994) divide alteration at mid-ocean ridges into three realms: axial, flank and basinal. The first realm occurs at the axis of mid-ocean ridges where high temperatures associated with magmatic cooling drive advection of vast quantities of seawater through the fresh basalt. The fluids exiting ridge axes have Mg/Ca of zero (Alt, 2003). The basinal realm is characterized by conductive cooling of the oceanic lithosphere and little hydrothermal movement of fluids, thus it plays a negligible role in the alteration of ridge material and has no effect on the oceanic Mg budget. However, he flank realm, intermediate between the axial and basinal realms, hydrothermal circulation is advective with fluids exiting this realm with an Mg/Ca = 0.2 mol/

mol.

From these fluxes, the effect of mid-ocean ridge accretion can be linked to oceanic Mg/Ca. When larger volumes of oceanic basalt are produced per unit time, there is a greater flux of seawater through the fresh basalt and oceanic Mg/Ca falls. Conversely, during times of less voluminous production of oceanic basalt per unit time, oceanic Mg/Ca rises. Since accretion of oceanic crust is interpreted to be the first-order control on sea-level, Sandberg (1983) synthesized a curve (Figure 1B, 1G) for the Phanerozoic secular variation in "calcite/aragonite seas" from the sea-level curves of Hallam (1977) and Vail et al. (1977).

Others have suggested that the formation of dolomite is the primary sink for oceanic Mg (e.g. Given and Wilkinson, 1987; Mackenzie and Pigott, 1981) throughout the Phanerozoic, even through mid-ocean ridge cation exchange reactions dominate today's Mg cycle (Wilkinson and Algeo, 1989). The dolomite sink operates as follows: sea-level highstands inundate continental margins, CO_2 is released into the atmosphere due to clay-carbonate mineral reactions. There is then a concomitant lowering oceanic pH, which enhances dissolution of calcite, and thus the precipitation of dolomite (provided an adequate supply of Mg exists).

The Sr budget in the modern ocean is controlled by two inputs, mid-ocean ridge volcanism (Alt, 2003) and the erosion of continental crust (Schlanger, 1988; Lear et al., 2003) and one output, carbonate precipitation (Steuber and Veizer, 1999). To change the Sr/Ca ratio of the ocean, one of these fluxes must be altered or the reservoir of oceanic Ca must change.

Today, mid-ocean ridge hydrothermal systems are characterized by a negligible flux of Sr at ridge axes and flank fluxes are on the order of 2.5×10^9 mol/yr with a Sr/Ca of 2 mmol/mol (Alt, 2003). An order of magnitude larger flux of Sr reaches the ocean by the erosion of continental crust (2-8 $\times 10^{10}$ mol/yr). According to Schlanger (1988), incorporation of Sr into aragonite phases is of minor importance since most is lost to interstitial fluids upon early diagenetic stabilization. This mechanism results in very little Sr leaving the oceanic reservoir. Steuber and Veizer (1999) suggest that this flux is non-trivial and that in fact approximately 50% of Sr

precipitated in carbonate phases does not return to the ocean.

Muleshoe marine cement has a very low value (0.15-0.2 mmol/mol $Sr/Ca_{calcite}$) compared to the average, brachiopod-derived Mississippian value of Steuber and Veizer (1999) of 0.9 mmol/mol $Sr/Ca_{calcite}$.

Dickson (2004) reported that fossil echinoderms can retain their bulk chemistry despite minor diagenetic alteration and thus are a viable proxy for ancient ocean chemistry. Degree of diagenetic alteration was qualitative, based on stereom preservation as viewed under SEM. No geochemical tests of diagenesis were performed. A calcite Mg partition coefficient (D_{Mg}) derived from modern echinoids was then applied to the fossil crinoids. The resulting seawater Mg/Ca values, while generally following the Mg/Ca trends of other workers, plot with error bars at least ± 0.5 mol/mol (i.e. >25% of the estimated Phanerozoic variation in seawater Mg/Ca) to a maximum of ± 1.5 mol/mol (i.e. 75%). In addition, when Dickson (2004) applied his calcite D_{Mg} to a modern echinoid, he obtained a seawater Mg/Ca = 1.8 mol/mol.

Morse et al. (1997) documented the role of temperature in the precipitation of abiotic carbonate phases from seawaters with various Mg/Ca. At temperatures below ~6°C, low-Mg calcite precipitates from seawater since lower temperatures reduce precipitation rates, allowing the calcite crystal to discriminate against Mg. Since most of today's ocean water is below 6°C, most of the ocean today is a "calcite sea". Only those waters above the 6°C isotherm are warm enough to support an "aragonite sea". In this light, debate about alternations between "calcite seas" and "aragonite seas" seems inaccurate and that the root of the matter is the volume of the oceans that are both physically and chemically conducive to the production of aragonite. Although this is problematic in several respects as well. First, if we accept that calcite and aragonite seas can coexist we must define their domains not simply in time, but in all three dimensions as well, since any of the factors listed above as controlling Mg distribution can thus affect the distribution of aragonite.

This temperature control on $CaCO_3$ polymorph is counterintuitive. "Aragonite seas" coincide

with climatic icehouses (i.e. when one would not expect abundant warm water) and "calcite seas" with climatic greenhouses. Thus it seems more likely that another factor (or factors) arbitrates "calcite/aragonite sea" modality.

Acknowledgements

The ever-present guidance of Kacey C Lohmann, advisor *par excellence*, was essential to the creation, crystallization, and completion of this project. The many kind visits of Bruce Wilkinson to my office and his kind words ensured the timely completion of this project. Matt Wasson and Liz Smith were indispensable field assistants on Muleshoe. As office colleagues, Matt, Liz, and Maria Marcano were second to none in helping me understand the finer points of carbonate diagenesis and the human condition. The many hours of patient tutelage from Ted Huston and Lora Wingate assisted greatly in sample preparation and analysis as well as data interpretation. The Scott Turner Fund for Research at the University of Michigan grants funds for the completion of this study. Speleothem cements were collected at more northerly Lake Valley Fm outcrops by Dr. Tracy Frank during fieldwork in the late 1990s.

References

Ahr WM, 1989. Sedimentary and tectonic controls on the development of an Early Mississippian carbonate ramp, Sacramento Mountains area, New Mexico. Crevello PD; Wilson JJ, Sarg JF; Read JF *Eds*. SEPM Special Publication **44**: 203-212.

Ahr WM, Stanton RJ Jr, 1996.Constituent composition of Early Mississippian carbonate buildups and their level-bottom equivalents, Sacramento Mountains, New Mexico. In: Strogen P, Somerville ID, Jones GL *Eds*. Geological Society Special Publications, **107**: 83-95.

Alt JC, 2003. Hydrothermal fluxes at mid-ocean ridges and on ridge flanks. *C. R. Geoscience* **335**: 853–864.

Berner RA, 1975. The role of magnesium in the crystal growth of calcite and aragonite from sea water. *Geochimica et Cosmochimica Acta* **39**: 489-504.

Brand U, Logan A, Hillerc N, Richardson J, 2003. Geochemistry of modern brachiopods: applications and implications for oceanography and paleoceanography. *Chemical Geology* **198**: 305– 334.

Brennan ST, Lowenstein TK, 2002. The major-ion composition of Silurian seawater. *Geochimica et Cosmochimica Acta* **66**(15): 2683–2700.

Brennan ST, Lowenstein TK, Horita J, 2004. Seawater chemistry and the advent of biocalcification. *Geology* **32**(6): 473–476. doi: 10.1130/G20251.1

Brezinski DK, 2000. Lower Mississippian trilobites from Southern New Mexico. *Journal of Paleontology* **74**(6): 1043-1064.

Carbonate diagenesis on the modern and ancient sea floor, meteoric diagenesis and diagenesis in the zone of mixed waters.

Carpenter SC, Lohmann KC, 1992. Sr/Mg ratios of modern marine calcite: empirical indicators of ocean chemistry and precipitation rate. *Geochimica et Cosmochimica Acta* **56**: 1837–1849.

Carpenter SC, Lohmann KC, Holden P, Walter LM, Huston TJ, Halliday AN, 1991. $\delta^{18}O$ values, $^{87}Sr/^{86}Sr$, and Sr/Mg ratios of Late Devonian abiotic marine calcite: Implications for the composition of ancient seawater. *Geochimica et Cosmochimica Acta* **56**: 1837–1849.

Choquette PW, James NP, 1990. Limestones—The Burial Diagenetic Environment. *In* Diagenesis, McIlreath and Morrow DW, *eds*: Diagenesis. 75-113.

Cicero AD, Lohmann KC, 2001. Sr/Mg variation during water-rock interaction: Implications for secular changes in the elemental chemistry of ancient seawater. *Geochimica et Cosmochimica Acta* **65**: 741–761.

Curti E, 1999. Coprecipitation of radionuclides with calcite: estimation of partition coeÅcients based on a review of laboratory investigations and geochemical data. *Applied Geochemistry* **14**: 433-445.

Davies GR, 1977. Former magnesian calcite and aragonite submarine cements in upper Paleozoic reefs of the Canadian Arctic: A summary. *Geology* **5**: 11-15.

Davis KJ, Dove PM, DeYoreo JJ, 2000. The role of Mg^{2+} as an impurity in calcite growth. *Science* **290**: 1134-1137.

Dickson JAD, 2004. Echinoderm skeletal preservation; calcite-aragonite seas and the Mg/Ca ratio of Phanerozoic oceans. *Journal of Sedimentary Research* **74**, 355-365.

Doerner HA, Hoskins WM, 1925. Co-Precipitation of Radium and Barium Sulfates. *Journal of the American Chemical Society* **47**: 662-675.

Douthit TL, 1990. Geochemical analysis of the Irish Waulsortian Limestone: implications for the strontium isotopic composition of Lower Carboniferous seawater. Unpublished MSc Thesis. State University of New York, Stony Brook.

Dubois P, 1990. Biological controls of skeleton properties in echinoderms. In *Echinoderm Research*, DeRidder, Dubois, Lahaye, Jangoux (eds): 17-22.

Emson RH, 1984. Bone idle—A recipe for success? Proceedings of the Fifth International Echinoderm Conference: 25-30.

Fischer AG, 1981. Climatic oscillations in the biosphere; Biotic crises in ecological and evolutionary time. M. Nitecki, ed. New York: Academic.

Folk RL, 1974. The natural history of crystalline calcium carbonate: effect of magnesium content and salinity. *Journal of Sedimentary Petrology* **44**(1): 40-53.

Frank TD, Lohmann KC, 1996. Diagenesis of fibrous magnesian calcite marine cement, implications for the interpretation of delta (super 18) O and delta (super 13) C values of ancient equivalents. *Geochimica et Cosmochimica Acta* **60**(13): 2427-2436.

Frank TD, Lohmann KC, Meyers WJ, 1996.Chronostratigraphic significance of cathodoluminescence zoning in syntaxial cement; Mississippian Lake Valley Formation, New Mexico. *Sedimentary Geology* **105**(1-2): 29-50

Freitas P, Clarke LJ, Kennedy H, Richardson C, Abrantes F, 2005. Mg/Ca, Sr/Ca, and stable-isotope ($\delta^{18}O$ and $\delta^{13}C$) ratio profiles from the fan mussel *Pinna nobilis*: Seasonal records and temperature relationships. *Geochemistry Geophysics Geosystems* **6**(4): Q04D14. doi:10.1029/2004GC000872

Fuchtbauer H, Hardie LA, 1976. Experimentally determined homogeneous distribution for precipitated magnesian calcites, application to marine carbonate cements. *Abstracts with*

Programs - Geological Society of America **8**(6): 877.

Gaffin S, 1987. Ridge volume dependence on seafloor generation rate and inversion using long term sealevel change. *American Journal of Science* **287**(6): 596-611.

Given RK, Wilkinson BH, 1986. Dolomite: abundance and stratigraphic age: constraints on rates and mechanisms of Phanerozoic dolostone formation. *Journal of Sedimentary Petrology* **57**(6), 1068-1078.

Gonzalez LA, Lohmann KC, 1985. Carbon and oxygen isotopic composition of Holocene reefal carbonates. *Geology* **13**(11): 811–814.

Gutjar A, Dabringhaus H, Lacmann R, 1996. Studies of the growth and dissolution kinetics of the $CaCO_3$ polymorphs calcite and aragonite II. The influence of divalent cation additives on the growth and dissolution rates. *Journal of Crystal Growth* **158**: 310-315.

Hallam A, 1984. Pre-Quaternary sea-level changes. *Annual Review of Earth and Planetary Sciences* **12**, 205-243.

Hardie LA, 1996. Secular variation in seawater chemistry; an explanation for the coupled secular variation in the mineralogies of marine limestones and potash evaporites over the past 600 m.y. *Geology (Boulder)* **24**, 279-283.

Horita J, Friedman TJ, Lazar B, Holland HD, 1991. The composition of Permian seawater. *Geochemica et Cosmochimica Acta* **55**: 417-432.

Horita J, Zimmermann H , Holland HD, 2002. Chemical evolution of seawater during the Phanerozoic: Implications from the record of marine evaporites. *Geochimica et Cosmochimica Acta* **66**(21): 3733–3756.

Horita J, Zimmermann H, Holland HD, 2002. Chemical evolution of seawater during the Phanerozoic: Implications from the record of marine evaporites. *Geochimica et Cosmochimica Acta* **66**(21): 3733–3756.

Kirkby KC, Hunt D, 1996. Episodic growth of a Waulsortian buildup: the Lower Carboniferous Muleshoe Mound, Sacramento Mountains, New Mexico, USA, *in* Strogen, P., Somerville, I.D., and Jones, G.L., eds., Recent Advances in Lower Carboniferous Geology: London, Geological Society (London) Special Publication **107**: 97-110.

Klein RT, Lohmann KC, Thayer CW, 1996. Sr/Ca and $^{13}C/^{12}C$ ratios in skeletal calcite of *Mytilus trossulus*: Covariation with metabolic rate, salinity, and carbon isotopic composition of seawater. *Geochimica et Cosmochimica Acta* **60**(21): 4207-4221.

Kohrt KA, 1988. Carbon and oxygen isotopic compositions of crinoids and calcite cements, Burlington-Keokuk formation (Mississippian), southeastern Iowa and western Illinois. Unpublished MSc Thesis. State University of New York, Stony Brook.

Kovalevich VM, Peryt TM, Petrichenko OI, 1998. Secular variation in seawater chemistry during the Phanerozoic as indicated by brine inclusions in halite. *Journal of Geology* **106**: 695-712.

Lear CH, Elderfield H, Wilson PA, 2003. A Cenozoic seawater Sr/Ca record from benthic foraminiferal calcite and its application in determining global weathering fluxes. *Earth and Planetary Science Letters* **208**: 69-84.

Leutloff AH, Meyers WJ, 1984. Regional distribution of microdolomite inclusions in Mississippian echinoderms from southwestern New Mexico. *Journal of Sedimentary Petrology* **54**(2): 432-446.

Lohmann KC, 1988. Geochemical patterns of meteoric diagenetic systems and their application to studies of paleokarst. In James NP, Choquette PW *(eds)* XXX, Springer-Verlag, New York: 58-80.

Lohmann KC, Meyers WJ, 1977. Microdolomite inclusions in cloudy prismatic calcites; a proposed criterion for former high-magnesium calcites. *Journal of Sedimentary Petrology* **47**(3): 1078-1088.

Lowenstein TK, Hardie LA, Timofeeff MN, Demicco RV, 2001. Secular variation in seawater chemistry and the origin of calcium chloride basinal brines. *Geology* **31**(10): 857–860.

Lowenstein TK, Timofeef MN, Brennan ST, Hardie LA, Demicco RV, 2001. Oscillations in Phanerozoic seawater chemistry: evidence from fluid inclusions. *Science* **294**: 1086-1088.

Mackenzie FT, Pigott JD, 1981. Tectonic controls of Phanerozoic sedimentary rock cycling. *Journal of the Geological Society of London* **138**: 183-196.

Macqueen RW, Ghent ED, 1974. Electron microprobe study of magnesium distribution in some Mississippian echinoderm limestones from western Canada. *Canadian Journal of Earth Sciences* **7**(5) 1308-1316.

Macqueen RW, Ghent ED, Davies GR, 1974. Magnesium distribution in living and fossil specimens of the echinoid *Peronella lesueuri* Agassiz, Shark Bay, Western Australia. *Journal of Sedimentary Petrology* **44**(1): 60-69.

Major RP, Wilber RJ, 1991. Crystal habit, geochemistry, and cathodoluminescence of magnesian calcite marine cements from the lower slope of the Little Bahama Bank. *GSA Bulletin* **103**: 461-471.

Meyers WJ, 1978. Carbonate cement stratigraphy of the Lake Valley Formation (Mississippian), Sacramento Mountains, New Mexico. *Journal of Sedimentary Petrology* **44**: 837-861.

Meyers WJ, Lohmann KC, 1978. Microdolomite-rich syntaxial cements; proposed meteoric-marine mixing zone phreatic cements from Mississippian limestones, New Mexico. *Journal of Sedimentary Petrology* **48**(2): 475-488.

Meyers WJ, Lohmann KC, 1985. Isotope geochemistry of regionally extensive calcite cement zones and marine components in the Mississippian limestones, New Mexico. *Special Publication-Society of Economic Paleontologists and Mineralogists* **36**: 223-239.

Mii H, Grossman EL, Yancey TE, 1999. Carboniferous isotope stratigraphies of North America: Implications for Carboniferous paleoceanography and Mississippian glaciation. *GSA Bulletin* **111**(7): 960–973.

Mitsuguchi T, Uchida T, MatsumotoE, Isdale PJ, Kawana T, 2001. Variations in Mg/Ca, Na/Ca, and Sr/Ca ratios of coral skeletons with chemical treatments: Implications for carbonate geochemistry. *Geochimica et Cosmochimica Acta* **65**(17): 2865–2874.

Morse JW, Wang Q, Tsio MY, 1997. Influences of temperature and Mg:Ca ratio on $CaCO_3$ precipitates from seawater. *Geology* **25**(1): 85–87.

Mottl MJ, Wheat CG, 1994. Hydrothermal circulation through mid-ocean ridge flanks: Fluxes of heat and magnesium. *Geochimica et Cosmochimica Acta* **58**(10): 2225-2237.

Mucci A, Morse JW, 1983. The incorporation of Mg^{2+} and Sr^{2+} into calcite overgrowths: influences of growth rate and solution composition. *Geochimica et Cosmochimica Acta* **47**: 217–233.

Pray LC, 1961, Geology of the Sacramento Mountains escarpment, Otero County, *New Mexico, New Mexico Bureau of Geology and Mineral Resources Bulletin* **35**. 144 p.

Rathbum AE, De Deckker P, 1997. Magnesium and strontium compositions of Recent benthic foraminifera from the Coral Sea, Australia and Prydz Bay, Antarctica. *Marine Micropaleontology* **32**: 231-248

Ries JB, 2004. Effect of ambient Mg/Ca ratio on Mg fractionation in calcareous marine invertebrates: A record of the oceanic Mg/Ca ratio over the Phanerozoic. *Geology* **32**(11): 981–984.

Rimstidt JD, Balog A, Webb J, 1998. Distribution of trace elements between carbonate minerals and aqueous solutions. *Geochimica et Cosmochimica Acta* **62**(11): 1851-1863.

Sandberg PA, 1975. New interpretations of Great Salt Lake ooids and of ancient non-skeletal carbonate mineralogy. *Sedimentology* **22**, 497-537.

Sandberg PA, 1983. An oscillating trend in Phanerozoic non-skeletal carbonate mineralogy. *Nature (London)* **305**, 19-22.

Schlager W, 2003. Benthic carbonate factories of the Phanerozoic. *International Journal of Earth Sciences* **92**(4): 445-464.

Schlanger SO, 1988. Strontium storage and release during deposition and diagenesis of marine carbonates related to sea-level variations. *NATO ASI Series. Series C: Mathematical and*

Physical Sciences **251**: 323-340.

Stanley SM, Hardie LA, 1998. Secular oscillations in the carbonate mineralogy of reef-building and sediment-producing organisms driven by tectonically forced shifts in seawater chemistry. *Palaeogeography, Palaeoclimatology, Palaeoecology* **144**, 3-19.

Steuber T, Veizer J, 2002. Phanerozoic record of plate tectonic control of seawater chemistry and carbonate sedimentation. *Geology* **30**(12): 1123-1126.

Takesue RK,Van Geen A, 2004. Mg/Ca, Sr/Ca, and stable isotopes in modern and Holocene *Protothaca staminea* shells from a northern California coastal upwelling region. *Geochimica et Cosmochimica Acta* **68**(19)845-3861. doi:10.1016/j.gca.2004.03.021

Thompson TG, Chow, TJ, 1955. The strontium-calcium atom ratio in carbonate secreting marine organisms. Papers in Marine Biology and Oceanography, Supplement to Volume 3 of Deep-Sea Research: 20-39.

Vail PR, Mitchum RM Jr, Thompson S III, 1977. Seismic stratigraphy and global changes of sea level; Part 4, Global cycles of relative changes of sea level; Seismic stratigraphy; applications to hydrocarbon exploration. *Memoir—American Association of Petroleum Geologists* 83-97.

Weber JN, 1968. Fractionation of the stable isotopes of carbon and oxygen in calcareous marine invertebrates—the Asteroidea, Ophiuroidea and Crinoidea. *Geochimica et Cosmochimica Acta* **32**: 33–70.

Weber JN, 1969. The incorporation of magnesium into the skeletal calcites of echinoderms. *American Journal of Science* **267**: 537–566.

Weber JN, Raup DM, 1966. Fractionation of the stable isotopes of carbon and oxygen in calcareous marine invertebrates—the Echinoidea. Variation of C^{13} and O^{18} content within individuals. *Geochimica et Cosmochimica Acta* **30**: 681–703.

Weber JN, Raup DM, 1966a. Fractionation of the stable isotopes of carbon and oxygen in marine calcareous organisms. The Echinoidea, Part 1, Variation of C^{13} and O^{18} content within individuals. *Geochimica et Cosmochimica Acta* **30**(7): 681-703.

Weber JN, Raup DM, 1966b. Fractionation of the stable isotopes of carbon and oxygen in marine calcareous organisms. The Echinoidea, Part 2, Environmental and genetic factors. *Geochimica et Cosmochimica Acta* **30**(7): 705-736.

Weber JN, Raup DM, 1968. Comparison of C^{13}/C^{12} and O^{18}/O^{16} in the skeletal calcite of Recent and fossil echinoids. *Journal of Paleontology* **42**(1): 37-50.

Wei G, Min S, Xianhua L, Baofu N, 2000. Mg/Ca, Sr/Ca and U/Ca ratios of a porites coral from Sanya Bay, Hainan Island, South China Sea and their relationships to sea surface temperature. *Palaeogeography, Palaeoclimatology, Palaeoecology* **162**: 59–74.

Wilkinson BH, Algeo TJ, 1987. Sedimentary carbonate record of calcium-magnesium cycling. *American Journal of Science* **289**:1158-1194.

Yu KF, Zhao JX, Weid GJ, Cheng XR, Chen TG, Felise T, Wang PX, Liu TS, 2005. $\delta^{18}O$, Sr/Ca and Mg/Ca records of *Porites lutea* corals from Leizhou Peninsula, northern South China Sea, and their applicability as paleoclimatic indicators. *Palaeogeography, Palaeoclimatology, Palaeoecology* **218**: 57– 73

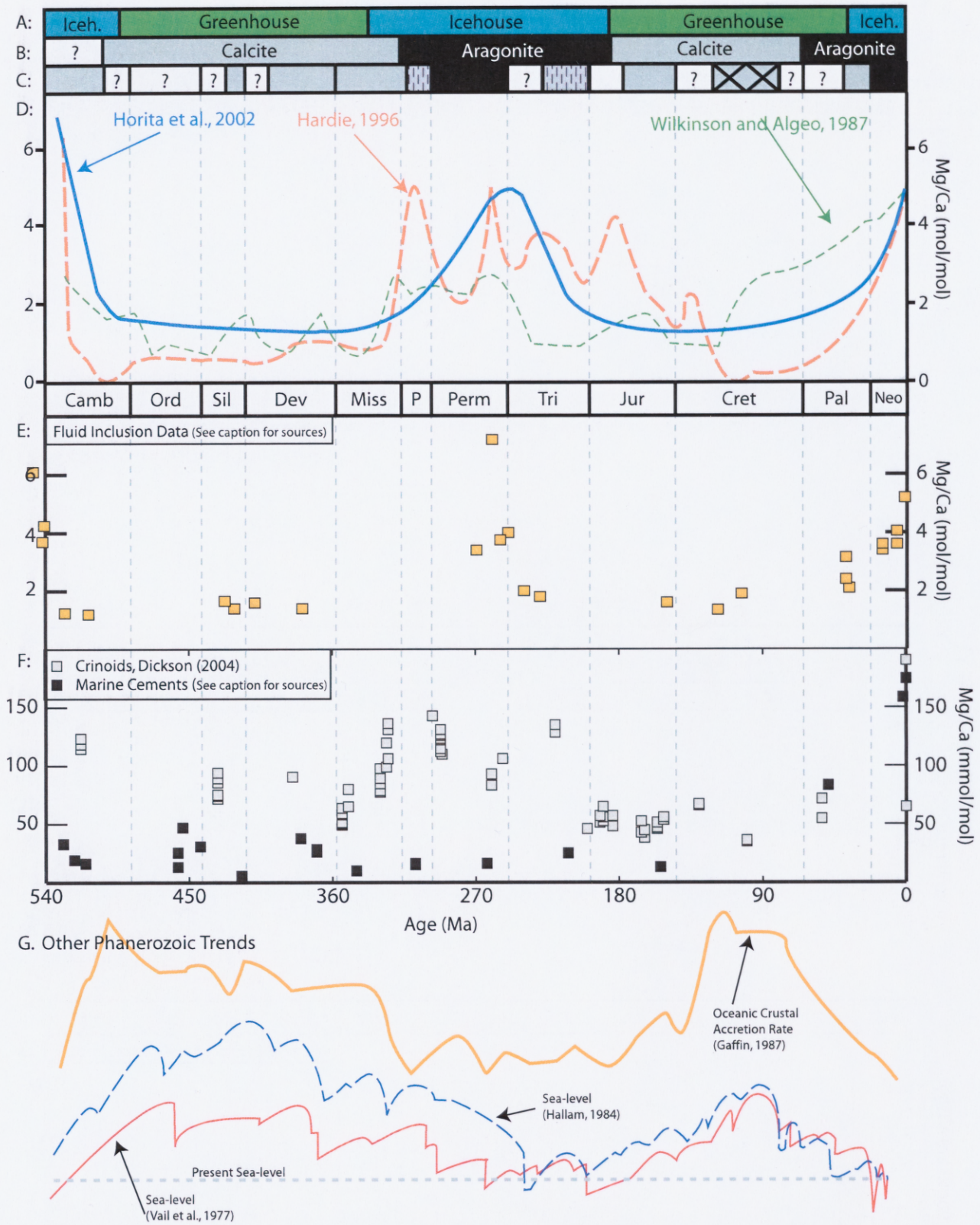

Figure 1. A: "Greenhouses" and "Icehouses" of Fischer (1981). **B:** "Aragonite Seas" and "Calcite Seas" of Sandberg (1983). **C: Phanerozoic** evaporite mineralogies of Kovalevich et al. (1998). Black represents $MgSO_4$ evaporites. Gray: KCl evaporites. Gray with Black Dots: KCl and $CaCl_2$ evaporites. Gray with Black Dashes: KCl and $MgSO_4$ evaporites. **D:** Phanerozoic Mg/Ca trends of Wilkinson and Algeo (1987), Hardie (1996), and Horita et al. (2002). **E:** Mg/Ca estimates derived from fluid inclusions (Horita et al, 1991; Lowenstein et al., 2001; Horita et al, 2002; Brenan and Lowenstein., 2002; Brennan et al., 2004). **F:** Mg/Ca estimates derived from Crinoids (Dickson, 2004) and marine cements (Benito et al., 2005; Cicero and Lohmann, 2001; Carpenter et al., 1991; Tobin et al., 1996; Tobin and Bergstrom, 2002; Whittaker et al., 1994; Davies 1976). **G:** Other Phanerozoic trends including oceanic crust accretion rate (Gaffin, 1987) and sea-level (Vail et al., 1977, and Hallam, 1984).

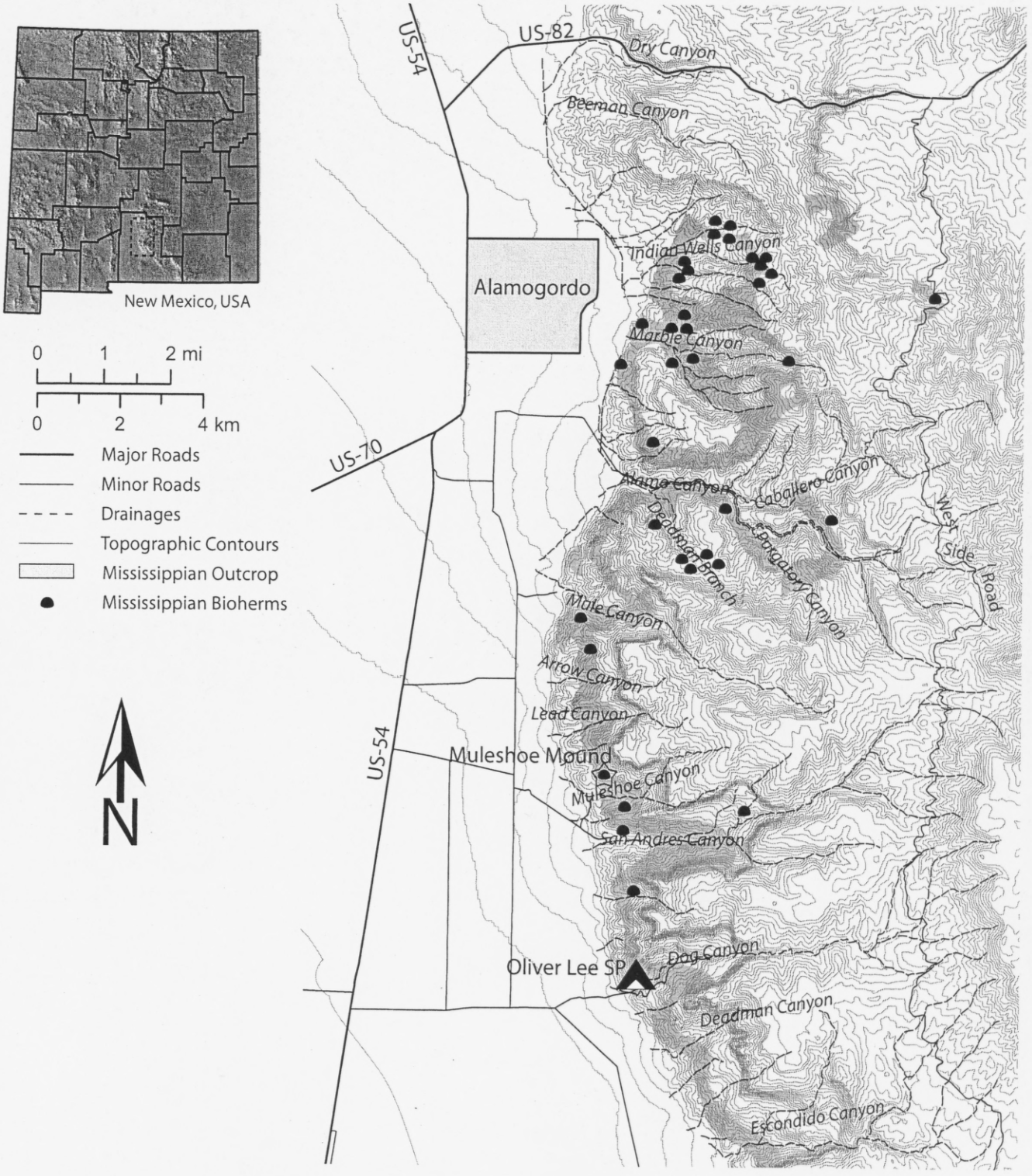

Figure 2. Location map of study area in the Sacramento Mountains, outside Alamogordo, New Mexico, USA. GIS data from New Mexico Resource GIS System. Bioherm locations from Ahr (1989).

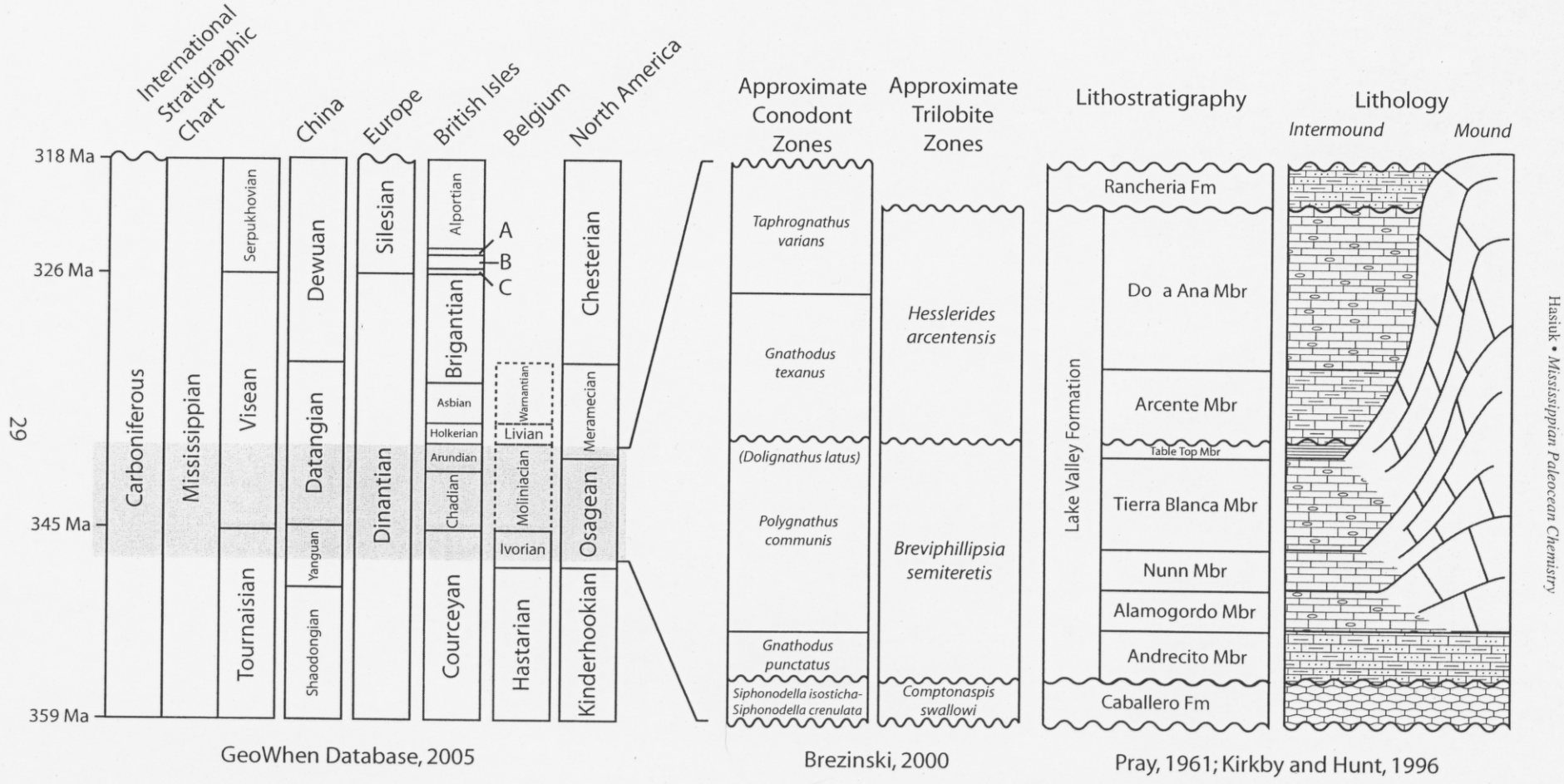

Figure 3. Stratigraphic section and correlation diagram for Muleshoe Mound. A: Chokierian. B: Arnsbergian. C: Pendleian.

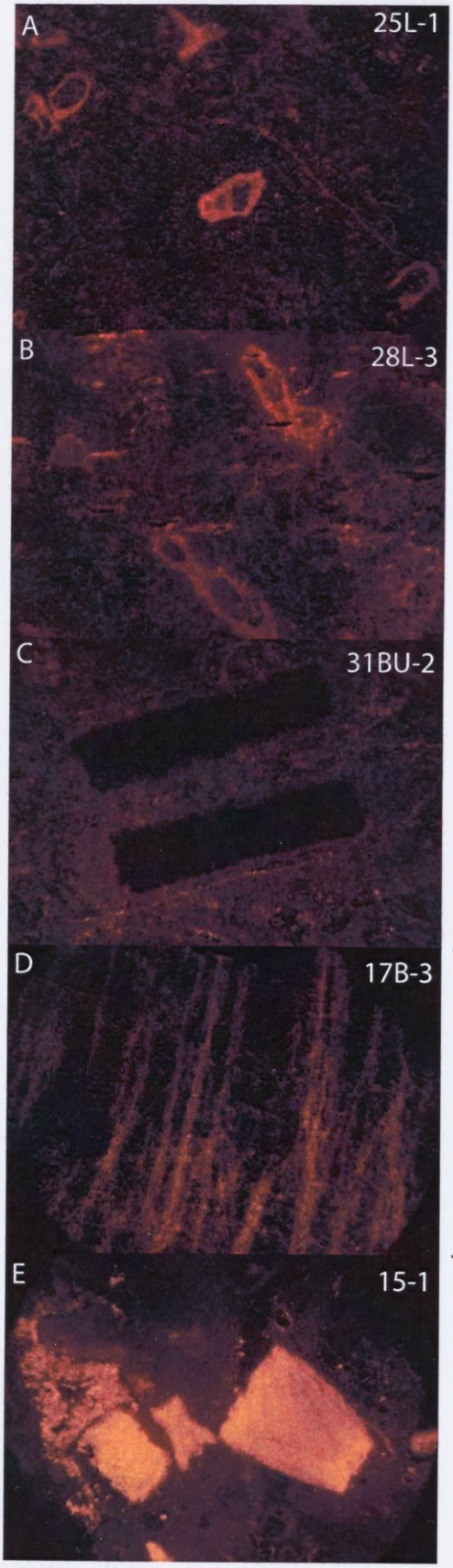

$\delta^{18}O$ = −1.69 ‰
$\delta^{13}C$ = +5.00 ‰
Mg/Ca = 9.04
Sr/Ca = 0.17
Mn/Ca = 0.12
Fe/Ca = 0.22

Non-luminescent cement surrounting luminescent bryozoan fragments. Geochemical data reinforce that this cement is relatively unaltered.

$\delta^{18}O$ = −5.95 ‰
$\delta^{13}C$ = +3.80 ‰
Mg/Ca = 8.722
Sr/Ca = 0.20
Mn/Ca = 0.24
Fe/Ca = 1.92

Non-luminescent cement surrounting luminescent fragments. Data suggest that this cement has been altered by burial diagensis.

$\delta^{18}O$ = −2.47 ‰
$\delta^{13}C$ = +4.69 ‰
Mg/Ca = 11.21
Sr/Ca = 0.17
Mn/Ca = 0.14
Fe/Ca = 0.30

Non-luminescent crinoid debris whose chemical composition is very similar to that of A.

$\delta^{18}O$ = −3.20 ‰
$\delta^{13}C$ = +4.81 ‰
Mg/Ca = 29.54
Sr/Ca = 0.24
Mn/Ca = 1.40
Fe/Ca = 0.12

Alternating luminescent/non-luminescent crinoid columnal (a "Tiger" crinoid). data suggest it has been somewhat altered.

$\delta^{18}O$ = −3.41 ‰
$\delta^{13}C$ = +4.56 ‰
Mg/Ca = 18.16
Sr/Ca = 0.28
Mn/Ca = 1.59
Fe/Ca = 0.61

Luminescent crinoid debris in a non-luminescent matrix. Data suggest that this debris has been altered.

Figure 4. Representative cathodoluminescence photomicrographs and geochemical data for most important analyzed phases.

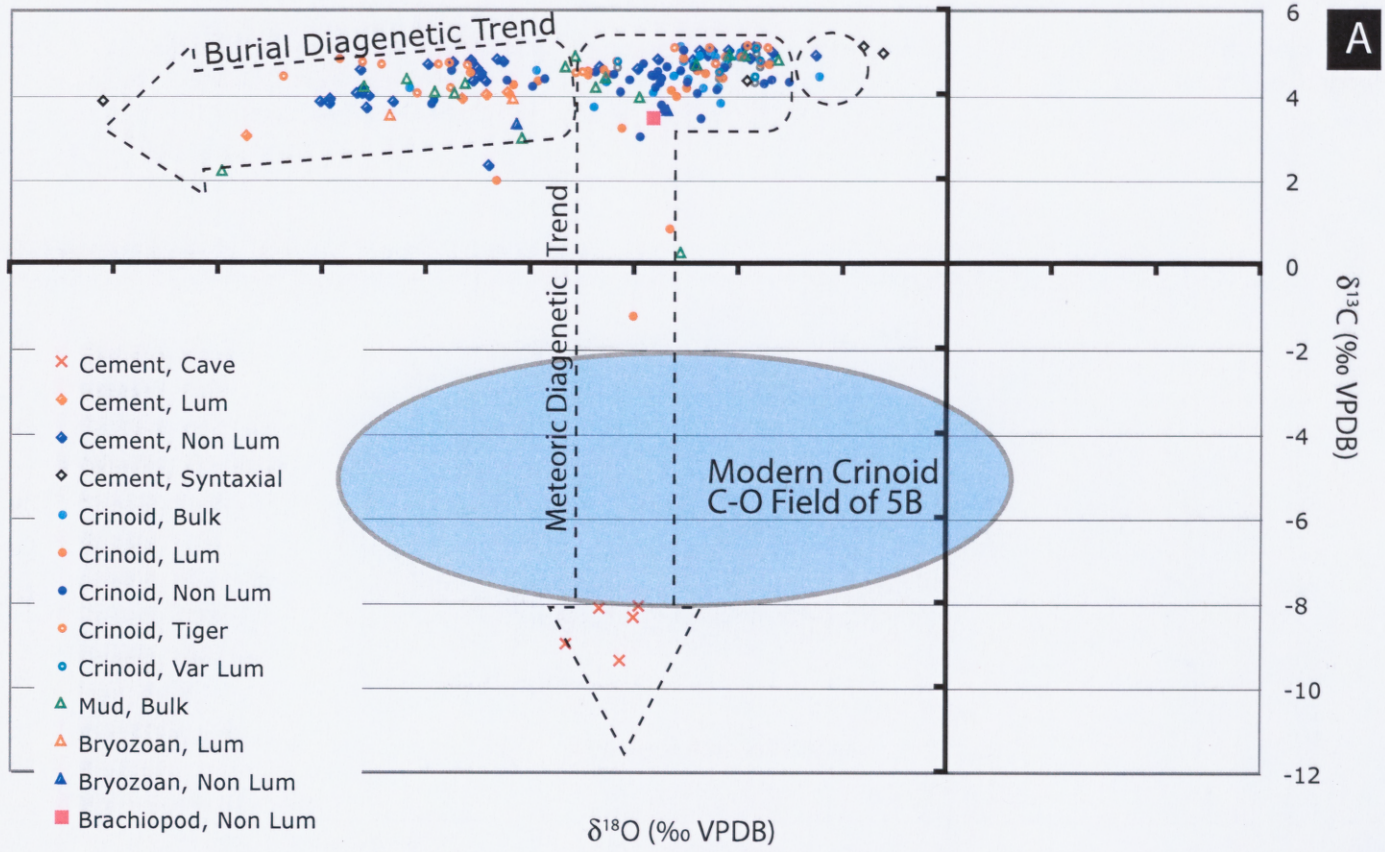

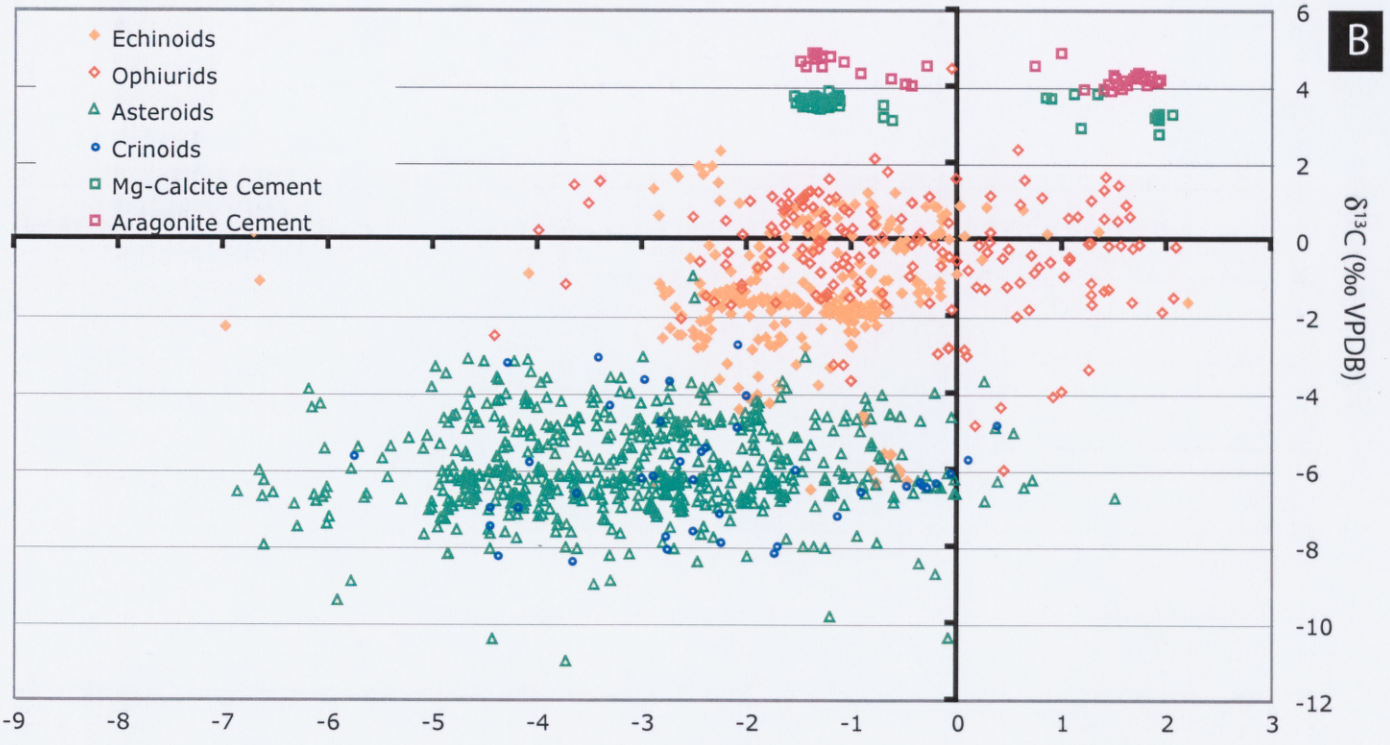

Figure 5. A: Stable isotope trends for Muleshoe marine cements, crinoids, and other material. Modern crinoids C-O field from 5A is plotted for reference. **B:** Stable isotope trends for modern marine cements (Gonzalez and Lohmann, 1985; Carpenter and Lohmann 1992) and modern echinoderms (Weber and Raup, 1965; Weber, 1968).

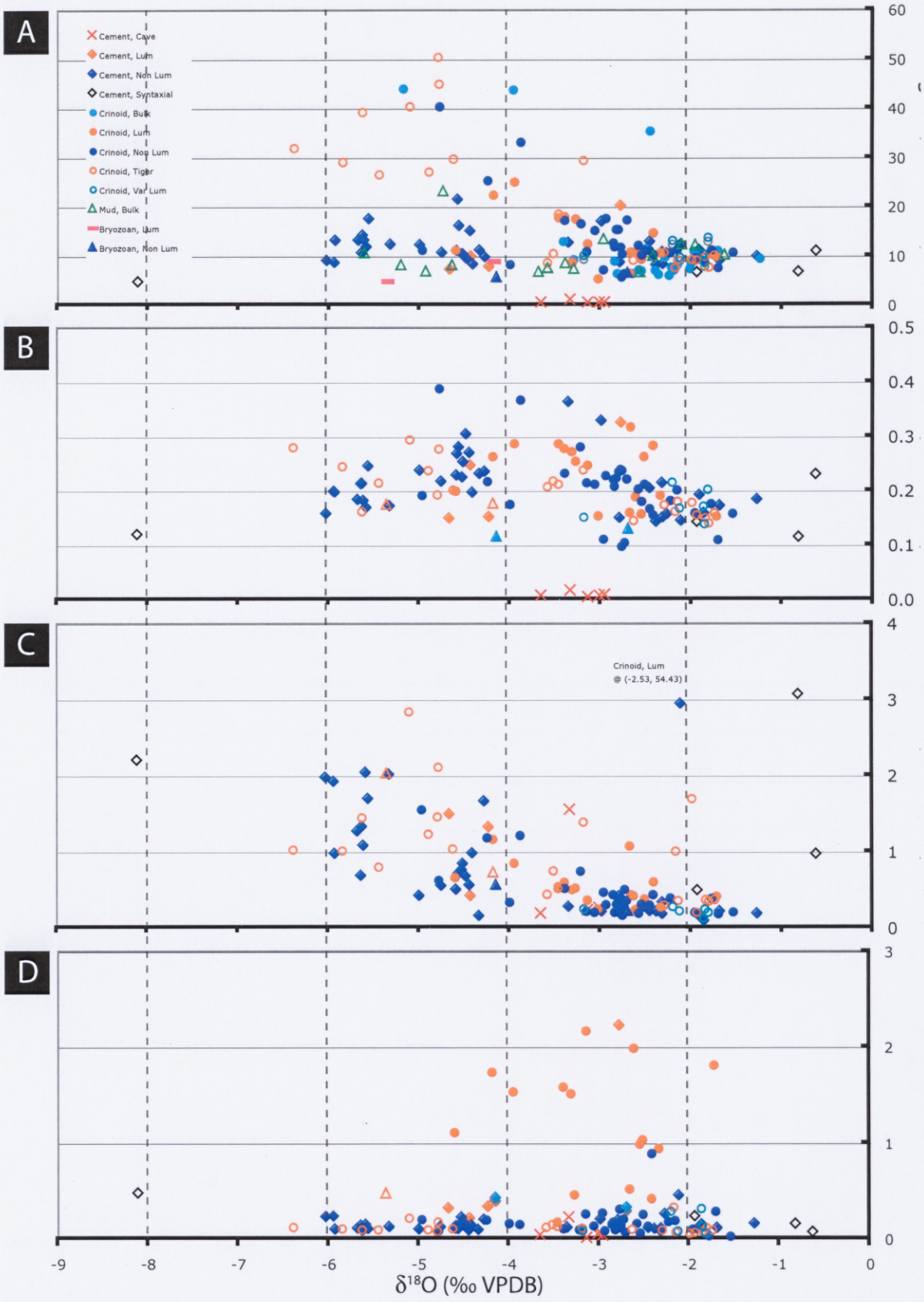

Figure 6. Cross-plots of the four elemental ratios against $\delta^{18}O$. **A:** Mg/Ca (mmol/mol). **B:** Sr/Ca (mmol/mol). **C:** Fe/Ca (mmol/mol). **D:** Mn/Ca (mmol/mol).

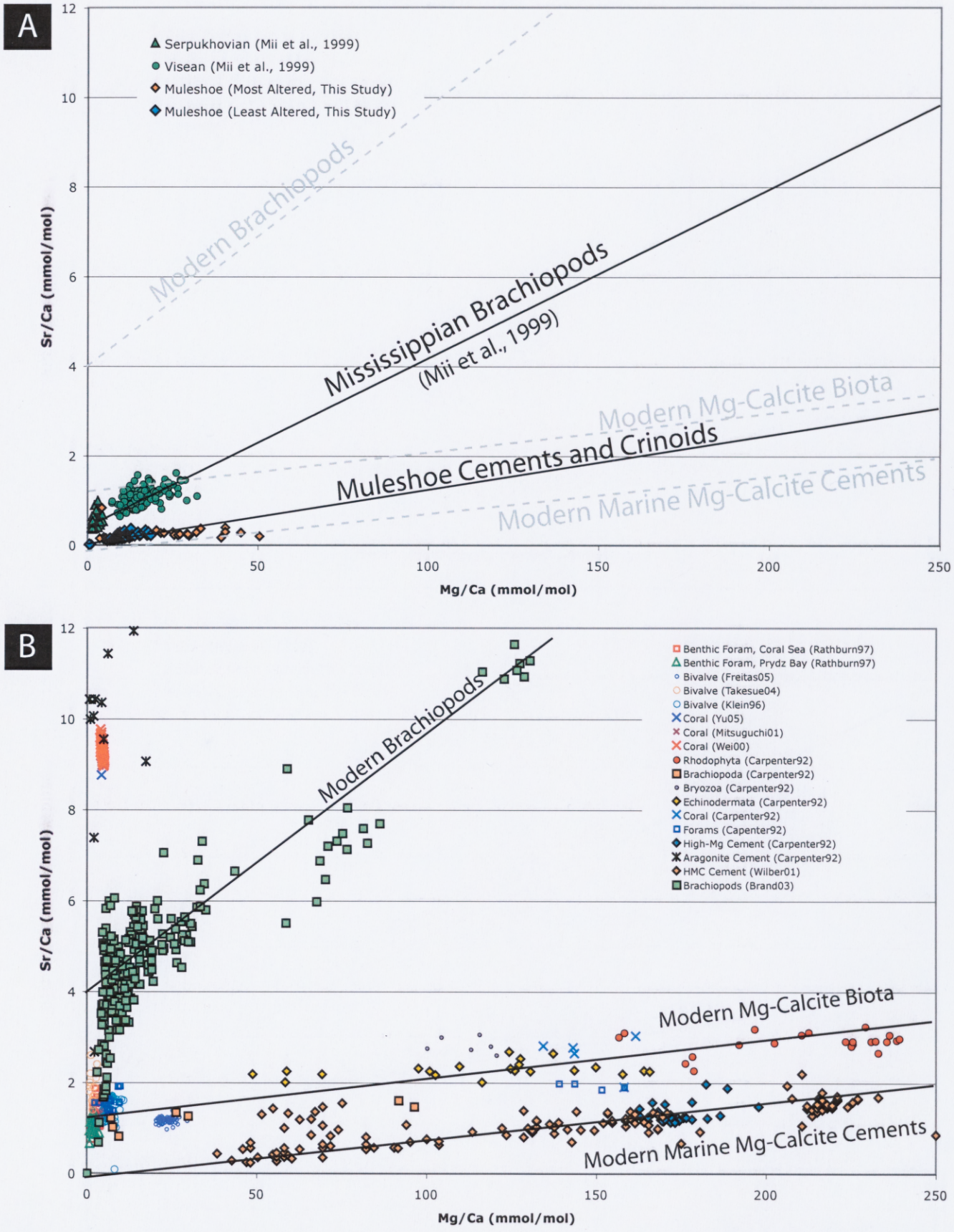

Figure 7. A: Sr/Ca-Mg/Ca trends for least-altered Muleshoe marine cements and crinoids as well as Mississippian brachiopods from the Russian Platform reported in Mii et al. (1999). **B:** Sr/Ca-Mg/Ca trends for modern marine magnesian calcite cements and modern biota (Brand et al., 2003; Rathburn and De Deckker, 1997; Freitas et al., 2005; Takesue and Van Geen, 2004; Klein et al., 1996; Mitsuguchi et al., 2001; Yu et al., 2005; Wei et al., 2000; Major and Wilber, 1991), which produce magnesian calcite.

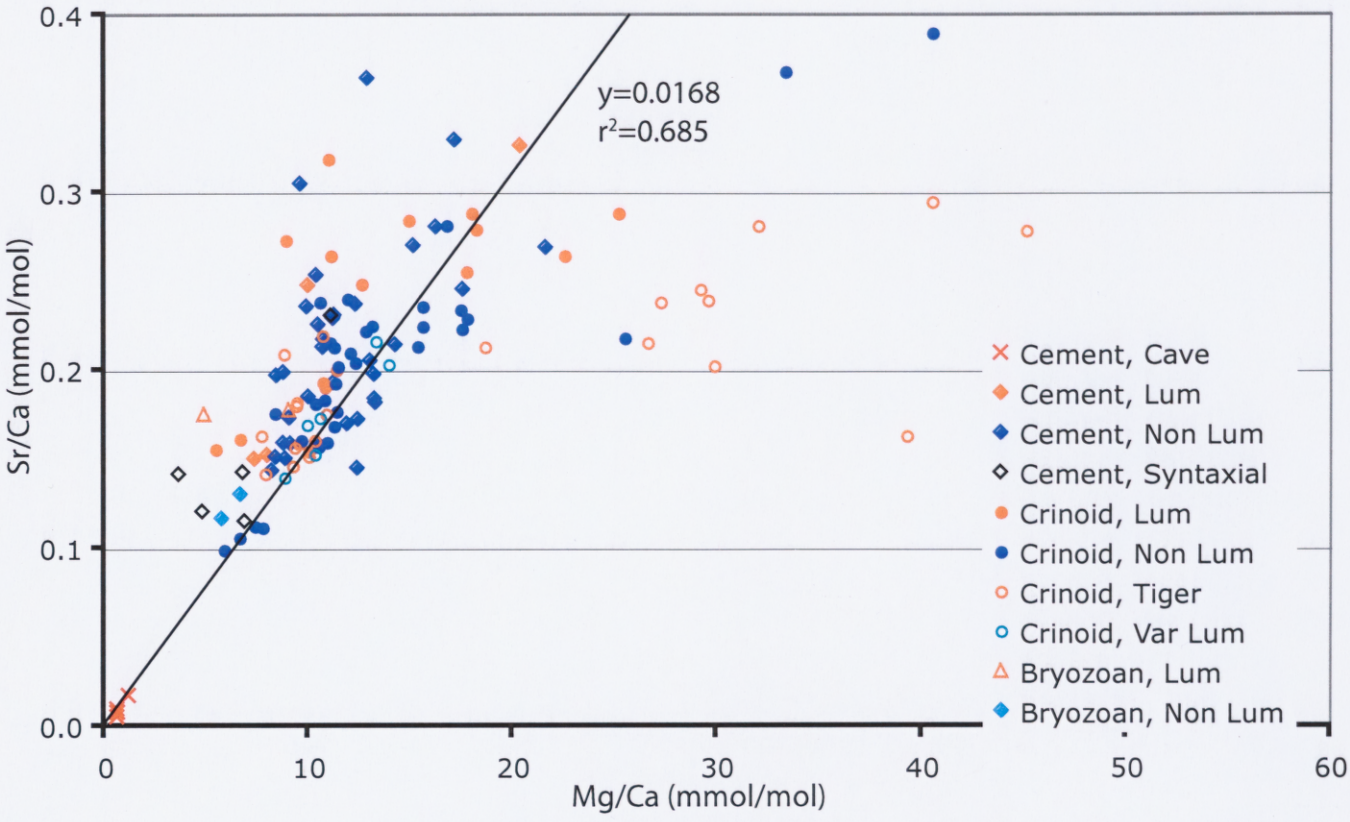

Figure 8. Mg/Ca-Sr/Ca crossplot. Regression line statistics are for data points (n=38) that pass geochemical tests for lack of diagenetic alteration. A number of "tiger" crinoid samples display Mg/Ca higher than is defined by the regression line.

Appendix 1: Isotopic and elemental data

Row	Sample	Site	EAST	NORTH	ELEV	Category	$\delta^{13}C$	$\delta^{18}O$	Mg/Ca	Sr/Ca	Fe/Ca	Mn/Ca	Sr/Mg	Mg+Sr	Fe/Mn	Fe+Mn	Ca	Mg	Sr	Mn	Fe
							(‰ VPDB)			(mmol/mol)								(ppm)			
1	01-1	F03	3705	9109	5162	Crinoid (B)	4.45	-1.26	9.54	-	0.39	0.04	0.035	9.87	10.05	0.43	397234	2298	81	21	215
2	01-2	F03	3705	9109	5162	Crinoid (B)	4.20	-2.23	7.80	-	0.33	0.09	0.047	8.16	3.78	0.42	397809	1881	88	48	182
3	02-1	F04	3825	9282	5313	Crinoid (B)	4.80	-1.72	11.25	-	0.77	0.14	0.052	11.84	5.35	0.92	396626	2706	140	79	428
4	02-2	F04	3825	9282	5313	Crinoid (B)	4.73	-2.17	8.26	-	0.28	0.05	0.046	8.64	5.74	0.33	397652	1991	92	27	157
5	03-1	F08	3818	9090	5408	Crinoid (B)	4.47	-2.66	6.50	-	0.72	0.34	0.085	7.05	2.14	1.06	398212	1569	133	184	400
6	03-2	F08	3818	9090	5408	Crinoid (B)	4.82	-2.56	7.12	-	0.39	0.18	0.080	7.69	2.17	0.57	398001	1718	137	98	217
7	05y-1	F10	3855	9071	5353	Crinoid (B)	4.93	-2.26	6.17	-	1.27	0.37	0.104	6.81	3.44	1.63	398307	1489	155	201	702
8	05y-2	F10	3855	9071	5353	Crinoid (B)	4.94	-2.41	7.20	-	0.52	0.84	0.073	7.72	0.62	1.36	397981	1737	127	460	289
9	06-1	F11	3844	9070	5374	Crinoid (B)	4.59	-3.98	43.90	-	2.96	0.30	0.022	44.87	9.94	3.26	386049	10279	226	158	1592
10	07-1	F13	3833	9137	5416	Crinoid (B)	4.76	-2.47	35.53	-	1.73	0.20	0.034	36.74	8.50	1.93	388654	8374	284	108	935
11	07-2	F13	3833	9137	5416	Crinoid (B)	4.20	-5.19	44.09	-	2.79	0.51	0.023	45.10	5.51	3.30	385983	10320	238	268	1503
12	08a-1	F14	3906	9190	5410	Crinoid (B)	4.52	-2.83	6.52	-	0.66	0.26	0.061	6.91	2.52	0.93	398230	1574	96	144	368
13	08B-1	F14	3906	9190	5410	Crinoid (B)	5.02	-2.01	8.64	-	1.29	0.45	0.082	9.35	2.85	1.74	397473	2082	171	246	714
14	08B-2	F14	3906	9190	5410	Crinoid (B)	4.92	-2.03	7.47	-	0.94	0.01	0.058	7.90	9.81	1.03	397906	1802	104	52	519
15	09-1	F15	3981	9165	5312	Crinoid (B)	5.05	-2.31	9.86	-	1.10	0.13	0.071	10.57	8.43	1.24	397066	2375	169	71	611
16	09-2	F15	3981	9165	5312	Crinoid (B)	5.17	-2.59	7.30	-	0.32	0.12	0.069	7.80	2.66	0.44	397951	1762	122	66	179
17	10-1	F16	4016	9075	5180	Crinoid (B)	4.18	-2.37	6.36	-	0.36	0.50	0.058	6.73	0.72	0.86	398287	1536	89	272	200
18	10-2	F16	4016	9075	5180	Crinoid (B)	4.08	-2.86	9.10	-	0.49	0.50	0.055	9.60	0.98	0.99	397352	2193	121	273	271
19	11-1	F17	4081	9053	5139	Crinoid (B)	4.40	-2.52	11.57	-	2.23	0.26	0.133	13.11	8.68	2.49	396366	2782	370	140	1232
20	11-2	F17	4081	9053	5139	Crinoid (B)	4.33	-3.31	9.40	-	0.54	0.16	0.130	10.63	3.48	0.69	397135	2265	295	84	299
21	13-1	F19	4084	9030	5095	Crinoid (B)	3.83	-2.21	7.26	-	2.88	0.01	0.038	7.54	29.48	2.97	398000	1753	67	53	1595
22	13-2	F19	4084	9030	5095	Crinoid (B)	3.75	-3.42	13.05	-	0.68	0.23	0.046	13.65	3.03	0.91	396029	3134	146	122	376
23	32-1	H18	3852	8934	4945	Crinoid (B)	4.91	-1.98	10.98	-	1.31	0.12	0.071	11.76	10.65	1.43	396683	2642	188	67	723
24	01-3	F03	3705	9109	5162	Micrite (B)	3.93	-2.97	13.43	-	1.75	0.34	0.027	13.80	5.14	2.09	395940	3226	89	185	967
25	02-3	F04	3825	9282	5313	Micrite (B)	4.81	-1.64	10.25	-	0.45	0.29	0.054	10.80	1.54	0.74	396964	2467	133	160	249
26	03-3	F08	3818	9090	5408	Micrite (B)	4.66	-3.69	6.86	-	6.88	0.39	0.061	7.28	17.66	7.27	398111	1656	101	213	3815
27	04-1	F09	3823	9079	5401	Micrite (B)	4.92	-1.96	12.31	-	2.43	0.18	0.058	13.03	13.84	2.61	396255	2958	172	96	1344
28	04-2	F09	3823	9079	5401	Micrite (B)	4.95	-2.11	12.36	-	0.80	0.14	0.059	13.09	5.70	0.94	396236	2971	174	76	440
29	04-3	F09	3823	9079	5401	Micrite (B)	4.26	-4.65	8.17	-	1.54	1.98	0.072	8.76	0.78	3.51	397648	1970	141	1077	851
30	05x-1	F10	3855	9071	5353	Micrite (B)	4.07	-4.93	6.95	-	1.73	0.63	0.104	7.67	2.77	2.36	398033	1677	174	341	961

Row	Sample	Site	EAST	NORTH	ELEV	Category	$\delta^{13}C$	$\delta^{18}O$	Mg/Ca	Sr/Ca	Fe/Ca	Mn/Ca	Sr/Mg	Mg+Sr	Fe/Mn	Fe+Mn	Ca	Mg	Sr	Mn	Fe
							(‰ VPDB)		(mmol/mol)								(ppm)				
31	05y-3	F10	3855	9071	5353	Micrite (B)	4.17	-3.39	8.59	-	0.87	1.07	0.072	9.21	0.81	1.94	397503	2071	149	584	479
32	05y-4	F10	3855	9071	5353	Micrite (B)	4.03	-4.75	23.23	-	2.16	0.68	0.033	23.99	3.20	2.84	392674	5531	181	364	1184
33	06-2	F11	3844	9070	5374	Micrite (B)	4.36	-5.21	8.18	-	1.10	0.48	0.091	8.92	2.30	1.58	397621	1972	179	261	610
34	07-3	F13	3833	9137	5416	Micrite (B)	4.18	-5.62	10.65	-	1.24	0.38	0.078	11.48	3.30	1.61	396785	2563	199	204	684
35	08B-3	F14	3906	9190	5410	Micrite (B)	2.20	-6.98	85.55	-	49.94	2.20	0.010	86.44	22.73	52.13	373429	19374	202	1125	25984
36	09-3	F15	3981	9165	5312	Micrite (B)	4.41	-3.30	7.42	-	0.96	0.70	0.080	8.01	1.37	1.66	397897	1791	142	382	532
37	10-3	F16	4016	9075	5180	Micrite (B)	0.28	-2.57	6.71	-	0.45	7.70	0.095	7.35	0.06	8.16	398127	1619	154	4204	251
38	12-1	F18	4095	9042	5122	Micrite (B)	2.97	-4.01	102.19	-	6.08	0.80	0.013	103.54	7.58	6.89	368547	22839	303	406	3124
39	32-2	H18	3852	8934	4945	Micrite (B)	4.90	-3.59	7.57	-	0.69	0.24	0.087	8.23	2.86	0.93	397836	1827	158	131	381
40	32-3	H18	3852	8934	4945	Micrite (B)	4.71	-2.43	10.09	-	0.27	0.17	0.103	11.13	1.61	0.43	396936	2430	250	90	148
41	20L-3	H06	3740	9122	5393	Bryozoan (L)	3.52	-5.36	4.87	0.18	2.03	0.48	0.036	5.05	4.23	2.51	398740	1178	153	263	1130
42	301-4	H16	3914	9002	5043	Bryozoan (L)	3.90	-4.19	9.02	0.18	0.73	0.41	0.020	9.20	1.80	1.14	397357	2173	155	221	404
43	131-1	F19	4084	9030	5095	Bryozoan (NL)	3.31	-4.15	5.74	0.12	0.57	0.43	0.020	5.85	1.31	1.00	398486	1386	102	237	315
44	131-7	F19	4084	9030	5095	Bryozoan (NL)	3.63	-2.70	6.62	0.13	0.22	0.34	0.020	6.75	0.66	0.56	398184	1598	114	184	123
45	CC-A	-	-	-	-	Cement (C)	-8.08	-2.96	0.61	0.001	-0.06	0.04	0.016	0.62	-1.52	-0.02	400270	147	9	21	0
46	CC-B	-	-	-	-	Cement (C)	-9.36	-3.15	0.61	0.005	0.23	0.01	0.009	0.62	17.23	0.25	400272	148	5	7	130
47	CC-C	-	-	-	-	Cement (C)	-8.97	-3.66	0.62	0.008	0.19	0.05	0.013	0.63	4.02	0.24	400267	150	7	26	105
48	CC-D	-	-	-	-	Cement (C)	-8.13	-3.34	1.16	0.017	1.56	0.23	0.015	1.18	6.85	1.78	400079	282	15	125	868
49	CC-E	-	-	-	-	Cement (C)	-8.35	-3.02	0.60	0.008	0.27	0.05	0.014	0.60	5.05	0.32	400275	144	7	29	148
50	012-3	F18	4095	9042	5122	Cement (L)	3.02	-6.74	-	-	-	-	-	-	-	-	-	-	-	-	-
51	16L-3A	H02	3546	9039	5709	Cement (L)	4.42	-2.78	20.32	0.326	0.18	2.23	0.016	20.64	0.08	2.41	393555	4849	281	1203	96
52	23L-3	H09	3807	9162	5431	Cement (L)	3.98	-4.44	9.93	0.248	0.42	0.22	0.025	10.18	1.91	0.64	397012	2392	215	120	234
53	25U-2B	H11	3832	9073	5396	Cement (L)	3.90	-4.67	7.34	0.150	1.50	0.32	0.021	7.49	4.62	1.82	397933	1770	131	177	830
54	25U-3B	H11	3832	9073	5396	Cement (L)	4.05	-4.24	7.95	0.153	1.33	0.34	0.019	8.10	3.93	1.66	397727	1918	133	184	735
55	071-1	F13	3833	9137	5416	Cement (NL)	3.97	-5.57	17.51	0.246	1.70	0.11	0.014	17.76	15.68	1.80	394517	4190	212	59	933
56	071-2	F13	3833	9137	5416	Cement (NL)	3.91	-5.94	13.16	0.198	0.97	0.10	0.015	13.36	9.47	1.07	395973	3161	172	56	536
57	071-3	F13	3833	9137	5416	Cement (NL)	4.03	-5.64	14.21	0.215	1.33	0.09	0.015	14.42	14.43	1.43	395619	3409	186	50	736
58	072-1	F13	3833	9137	5416	Cement (NL)	4.32	-4.45	15.09	0.270	0.56	0.01	0.018	15.36	5.88	0.66	395297	3617	234	52	309
59	072-2	F13	3833	9137	5416	Cement (NL)	4.32	-4.57	16.19	0.281	0.71	0.11	0.017	16.47	6.58	0.82	394929	3878	243	59	391
60	16L-1	H02	3546	9039	5709	Cement (NL)	4.51	-4.49	9.57	0.305	0.68	0.16	0.032	9.87	4.36	0.84	397100	2305	265	85	376
61	16L-2	H02	3546	9039	5709	Cement (NL)	4.65	-3.36	12.81	0.364	0.28	0.12	0.028	13.18	2.22	0.40	395993	3077	315	68	153

Row	Sample	Site	EAST	NORTH	ELEV	Category	$\delta^{13}C$ (‰ VPDB)	$\delta^{18}O$ (‰ VPDB)	Mg/Ca (mmol/mol)	Sr/Ca (mmol/mol)	Fe/Ca (mmol/mol)	Mn/Ca (mmol/mol)	Sr/Mg	Mg+Sr	Fe/Mn	Fe+Mn	Ca (ppm)	Mg (ppm)	Sr (ppm)	Mn (ppm)	Fe (ppm)
62	16L-3B	H02	3546	9039	5709	Cement (NL)	4.61	-2.99	17.01	0.330	0.21	0.21	0.019	17.43	1.02	0.42	394605	4091	284	112	116
63	16U-1	H02	3546	9039	5709	Cement (NL)	4.44	-4.52	10.34	0.254	0.85	0.18	0.025	10.59	4.69	1.03	396875	2488	220	98	467
64	18L-2	H04	3735	9133	5401	Cement (NL)	4.85	-1.92	11.20	0.194	0.15	0.11	0.017	11.40	1.39	0.26	396624	2694	168	59	84
65	18L-3	H04	3735	9133	5401	Cement (NL)	4.82	-2.46	12.97	0.206	0.22	0.12	0.016	13.17	1.88	0.34	396034	3114	178	64	123
66	18U-6	H04	3735	9133	5401	Cement (NL)	4.92	-2.33	10.84	0.22	0.18	0.08	0.020	11.06	2.13	0.26	396731	2608	187	46	99
67	23L-1	H09	3807	9162	5431	Cement (NL)	2.33	-4.42	8.38	0.198	0.98	0.15	0.024	8.57	6.67	1.13	397559	2020	172	80	543
68	25L-1	H11	3832	9073	5396	Cement (NL)	5.00	-1.69	9.04	0.174	0.22	0.12	0.019	9.21	1.87	0.34	397354	2177	151	64	122
69	25L-2	H11	3832	9073	5396	Cement (NL)	4.92	-1.28	9.96	0.185	0.19	0.16	0.019	10.14	1.15	0.35	397042	2397	161	89	105
70	25U-2	H11	3832	9073	5396	Cement (NL)	5.12	-1.87	8.75	0.160	0.01	0.15	0.018	8.91	0.63	0.25	397457	2109	139	84	54
71	25U-2A	H11	3832	9073	5396	Cement (NL)	5.04	-2.28	10.53	0.158	5.53	0.27	0.015	10.69	20.86	5.79	396867	2534	137	144	3056
72	25U-3A	H11	3832	9073	5396	Cement (NL)	4.83	-2.80	8.82	0.151	0.41	0.20	0.017	8.97	2.06	0.61	397438	2127	131	109	229
73	27L-1	H13	3835	9088	5411	Cement (NL)	4.62	-4.53	10.43	0.226	0.76	0.23	0.022	10.65	3.35	0.99	396862	2510	196	124	421
74	27L-2	H13	3835	9088	5411	Cement (NL)	4.79	-4.28	9.87	0.236	1.67	0.20	0.024	10.10	8.16	1.87	397042	2376	205	111	922
75	27L-3	H13	3835	9088	5411	Cement (NL)	4.81	-4.60	11.15	0.230	0.50	0.11	0.021	11.38	4.62	0.61	396621	2681	199	59	278
76	27L-5	H13	3835	9088	5411	Cement (NL)	4.84	-4.34	11.21	0.232	0.15	0.10	0.021	11.44	1.54	0.26	396601	2695	201	55	85
77	27U-1	H13	3835	9088	5411	Cement (NL)	4.58	-5.65	10.64	0.213	0.69	0.14	0.020	10.86	4.78	0.83	396798	2561	185	78	379
78	27U-2	H13	3835	9088	5411	Cement (NL)	4.79	-4.59	21.58	0.269	7.67	0.14	0.012	21.85	55.57	7.81	393177	5145	231	74	4201
79	27U-3	H13	3835	9088	5411	Cement (NL)	4.71	-5.00	12.25	0.238	0.42	0.11	0.019	12.48	3.94	0.53	396253	2943	206	58	232
80	27U-4	H13	3835	9088	5411	Cement (NL)	4.77	-4.76	10.68	0.218	0.55	0.13	0.020	10.90	4.25	0.68	396782	2571	189	71	306
81	28L-1	H14	3833	9127	5416	Cement (NL)	3.83	-5.33	12.37	0.173	2.02	0.13	0.014	12.54	15.67	2.15	396250	2972	150	70	1116
82	28L-2	H14	3833	9127	5416	Cement (NL)	3.69	-5.59	11.86	0.171	2.05	0.15	0.014	12.03	13.28	2.20	396420	2851	148	84	1130
83	28L-3	H14	3833	9127	5416	Cement (NL)	3.80	-5.95	8.73	0.199	1.92	0.24	0.023	8.92	8.07	2.16	397442	2103	173	130	1066
84	28U-1	H14	3833	9127	5416	Cement (NL)	3.83	-6.04	9.08	0.159	1.98	0.24	0.018	9.24	8.40	2.21	397347	2188	138	128	1095
85	28U-2	H14	3833	9127	5416	Cement (NL)	4.04	-5.69	13.20	0.185	1.27	0.11	0.014	13.38	11.18	1.38	395971	3169	160	62	701
86	28U-3	H14	3833	9127	5416	Cement (NL)	4.16	-5.62	13.24	0.182	1.08	0.10	0.014	13.42	10.63	1.18	395958	3179	158	55	597
87	321-1	H18	3852	8934	4945	Cement (NL)	4.94	-2.32	8.35	0.152	0.33	0.12	0.018	8.51	2.89	0.45	397593	2014	132	63	184
88	321-2	H18	3852	8934	4945	Cement (NL)	5.06	-2.12	12.36	0.146	2.95	0.46	0.012	12.51	6.44	3.41	396269	2971	126	249	1630
89	321-3	H18	3852	8934	4945	Cement (NL)	5.03	-2.39	8.17	0.144	0.21	0.11	0.018	8.31	1.96	0.32	397660	1969	125	59	117
90	011-2	F03	3705	9109	5162	Cement (S)	4.97	-0.63	11.07	0.23	0.98	0.08	0.021	11.30	12.77	1.05	396646	2663	201	42	540
91	091-1S	F15	3981	9165	5312	Cement (S)	5.13	-0.82	6.84	0.12	3.07	0.16	0.017	6.96	19.39	3.23	398118	1652	101	87	1705
92	092-3S	F15	3981	9165	5312	Cement (S)	4.34	-1.94	6.74	0.14	0.50	0.24	0.021	6.89	2.07	0.74	398135	1628	125	131	275

Row	Sample	Site	EAST	NORTH	ELEV	Category	$\delta^{13}C$	$\delta^{18}O$	Mg/Ca	Sr/Ca	Fe/Ca	Mn/Ca	Sr/Mg	Mg+Sr	Fe/Mn	Fe+Mn	Ca	Mg	Sr	Mn	Fe
							(‰ VPDB)		(mmol/mol)								(ppm)				
93	18U-2	H04	3735	9133	5401	Cement (S)	3.84	-8.12	4.78	0.12	2.21	0.48	0.025	4.90	4.63	2.69	398804	1156	105	261	1228
94	131-2	F19	4084	9030	5095	Cement (S)	-	-	3.61	0.14	2.06	0.91	0.039	3.75	2.26	2.98	399183	874	124	499	1148
95	071-1	F13	3833	9137	5416	Crinoid (L)	4.34	-3.96	25.15	0.29	0.86	1.54	0.011	25.43	0.56	2.40	394517	4190	212	59	933
96	071-2	F13	3833	9137	5416	Crinoid (L)	4.27	-4.20	22.51	0.26	1.17	1.75	0.012	22.78	0.67	2.91	395973	3161	172	56	536
97	091-2	F15	3981	9165	5312	Crinoid (L)	4.89	-2.56	9.50	0.16	54.43	1.00	0.017	9.66	54.52	55.43	397207	2289	138	544	30126
98	092-2	F15	3981	9165	5312	Crinoid (L)	4.74	-1.74	9.98	0.16	0.42	1.82	0.016	10.14	0.23	2.24	397050	2404	135	992	232
99	101-4	F16	4016	9075	5180	Crinoid (L)	0.87	-2.69	6.64	0.16	1.08	7.22	0.024	6.80	0.15	8.30	398160	1602	141	3941	599
100	101-6	F16	4016	9075	5180	Crinoid (L)	-1.19	-3.04	5.45	0.16	0.25	13.12	0.029	5.61	0.02	13.37	398558	1318	136	7167	140
101	111-2	F17	4081	9053	5139	Crinoid (L)	4.19	-2.53	11.07	0.26	0.39	1.04	0.024	11.34	0.37	1.43	396626	2663	229	568	213
102	111-4	F17	4081	9053	5139	Crinoid (L)	4.14	-2.68	10.94	0.32	0.44	0.53	0.029	11.26	0.83	0.97	396638	2631	277	289	245
103	15-1	H01	3778	9149	5438	Crinoid (L)	4.56	-3.41	18.16	0.28	0.61	1.59	0.015	18.44	0.38	2.20	394286	4342	241	859	333
104	18U-1	H04	3735	9133	5401	Crinoid (L)	4.62	-3.33	8.87	0.27	0.51	1.52	0.031	9.14	0.34	2.03	397351	2138	237	829	282
105	18U-4	H04	3735	9133	5401	Crinoid (L)	4.61	-2.43	14.88	0.28	0.61	0.43	0.019	15.16	1.43	1.04	395360	3567	246	232	337
106	19-3	H05	3734	9122	5359	Crinoid (L)	4.50	-3.48	17.95	0.29	0.55	0.19	0.016	18.24	2.92	0.73	394350	4292	249	101	300
107	19-5	H05	3734	9122	5359	Crinoid (L)	4.55	-4.61	11.36	0.20	0.67	1.12	0.018	11.56	0.60	1.79	396568	2732	174	608	369
108	20L-2	H06	3740	9122	5393	Crinoid (L)	4.50	-3.29	17.70	0.26	0.53	0.47	0.014	17.96	1.12	1.00	394450	4234	220	254	290
109	20L-6	H06	3740	9122	5393	Crinoid (L)	2.00	-4.35	-	-	-	-	-	-	-	-	-	-	-	-	-
110	31AU-5	H17	3885	8960	4966	Crinoid (L)	4.54	-2.35	10.69	0.19	0.28	0.95	0.018	10.88	0.29	1.23	396795	2572	168	518	153
111	31BU-3	H17	3885	8960	4966	Crinoid (L)	3.99	-2.63	10.77	0.19	0.25	2.00	0.018	10.96	0.12	2.24	396769	2591	166	1085	137
112	31BU-8	H17	3885	8960	4966	Crinoid (L)	3.25	-3.16	12.58	0.25	0.37	2.18	0.020	12.83	0.17	2.55	396136	3022	216	1183	204
113	011-1	F03	3705	9109	5162	Crinoid (NL)	4.34	-1.55	10.88	0.16	0.21	0.04	0.015	11.04	5.71	0.25	396751	2617	139	20	118
114	012-2	F03	3705	9109	5162	Crinoid (NL)	4.30	-1.79	11.34	0.18	0.39	0.04	0.016	11.52	10.01	0.43	396588	2727	154	21	216
115	092-1R	F15	3981	9165	5312	Crinoid (NL)	5.16	-1.97	9.63	0.16	0.21	0.11	0.017	9.79	1.92	0.32	397163	2320	140	59	116
116	101-5	F16	4016	9075	5180	Crinoid (NL)	4.06	-2.43	10.45	0.16	0.44	0.90	0.015	10.61	0.49	1.34	396894	2516	137	490	243
117	101-7	F16	4016	9075	5180	Crinoid (NL)	4.39	-1.72	7.74	0.11	0.19	0.29	0.014	7.85	0.65	0.48	397820	1868	97	160	106
118	111-1	F17	4081	9053	5139	Crinoid (NL)	4.43	-2.77	10.52	0.24	0.17	0.15	0.023	10.76	1.16	0.32	396825	2531	207	81	96
119	111-3	F17	4081	9053	5139	Crinoid (NL)	-	-	13.08	0.23	0.50	0.28	0.017	13.31	1.82	0.78	395984	3142	195	149	276
120	131-3	F19	4084	9030	5095	Crinoid (NL)	3.80	-2.78	5.85	0.10	0.28	0.13	0.017	5.95	2.22	0.41	398459	1413	87	69	156
121	131-4	F19	4084	9030	5095	Crinoid (NL)	3.47	-2.40	-	-	-	-	-	-	-	-	-	-	-	-	-
122	131-5	F19	4084	9030	5095	Crinoid (NL)	3.05	-2.98	7.36	0.11	0.47	0.28	0.015	7.47	1.69	0.75	397948	1775	98	153	263
123	131-6	F19	4084	9030	5095	Crinoid (NL)	3.67	-2.75	6.59	0.11	0.51	0.21	0.016	6.69	2.37	0.72	398209	1590	92	117	282

Row	Sample	Site	EAST	NORTH	ELEV	Category	$\delta^{13}C$	$\delta^{18}O$	Mg/Ca	Sr/Ca	Fe/Ca	Mn/Ca	Sr/Mg	Mg+Sr	Fe/Mn	Fe+Mn	Ca	Mg	Sr	Mn	Fe
							(‰ VPDB)		(mmol/mol)								(ppm)				
124	15-2	H01	3778	9149	5438	Crinoid (NL)	4.60	-4.79	40.53	0.39	0.63	0.01	0.001	40.92	6.58	0.73	387043	9512	330	51	340
125	15-3	H01	3778	9149	5438	Crinoid (NL)	4.51	-3.23	16.73	0.28	0.75	0.11	0.017	17.01	7.07	0.85	394754	4004	243	57	411
126	15-4	H01	3778	9149	5438	Crinoid (NL)	4.40	-3.89	33.31	0.37	1.22	0.16	0.011	33.68	7.53	1.38	389342	7866	313	86	661
127	19-2	H05	3734	9122	5359	Crinoid (NL)	4.69	-2.72	17.47	0.22	0.37	0.08	0.013	17.70	4.57	0.45	394542	4181	193	43	201
128	19-4	H05	3734	9122	5359	Crinoid (NL)	5.08	-2.56	10.29	0.18	0.32	0.07	0.018	10.48	4.61	0.38	396932	2478	158	37	174
129	19-6	H05	3734	9122	5359	Crinoid (NL)	4.37	-4.26	25.45	0.22	1.19	0.21	0.009	25.66	5.76	1.39	391951	6049	187	111	649
130	20L-1	H06	3740	9122	5393	Crinoid (NL)	4.56	-3.41	17.41	0.23	0.52	0.12	0.013	17.65	4.52	0.64	394556	4167	202	62	286
131	20L-4	H06	3740	9122	5393	Crinoid (NL)	3.81	-4.98	11.30	0.19	1.56	0.21	0.017	11.49	7.40	1.77	396593	2717	168	115	864
132	20L-9	H06	3740	9122	5393	Crinoid (NL)	3.91	-4.96	-	-	-	-	-	-	-	-	-	-	-	-	-
133	301-1	H16	3914	9002	5043	Crinoid (NL)	4.21	-2.84	15.56	0.22	0.31	0.11	0.014	15.78	2.95	0.42	395171	3728	194	58	173
134	31AU-1L	H17	3885	8960	4966	Crinoid (NL)	4.16	-2.24	10.75	0.18	0.40	0.19	0.017	10.93	2.08	0.59	396780	2586	159	104	220
135	31AU-1U	H17	3885	8960	4966	Crinoid (NL)	4.68	-2.17	11.40	0.20	4.61	0.20	0.018	11.60	22.82	4.81	396555	2741	176	110	2548
136	31AU-2R	H17	3885	8960	4966	Crinoid (NL)	4.23	-4.01	8.34	0.18	0.34	0.17	0.021	8.52	2.03	0.51	397583	2011	153	92	189
137	31AU-2T	H17	3885	8960	4966	Crinoid (NL)	4.77	-2.95	17.72	0.23	0.31	0.01	0.013	17.95	3.25	0.41	394458	4239	198	52	171
138	31AU-3	H17	3885	8960	4966	Crinoid (NL)	4.33	-2.53	11.21	0.21	0.28	0.26	0.019	11.42	1.05	0.54	396611	2695	185	144	153
139	31AU-4	H17	3885	8960	4966	Crinoid (NL)	4.11	-3.17	11.03	0.22	0.22	0.27	0.020	11.24	0.82	0.49	396669	2653	187	146	121
140	31AU-6	H17	3885	8960	4966	Crinoid (NL)	4.32	-2.79	11.89	0.24	0.31	0.32	0.020	12.13	0.96	0.62	396369	2859	208	173	169
141	31BU-1	H17	3885	8960	4966	Crinoid (NL)	4.60	-2.59	12.27	0.20	0.20	0.17	0.017	12.47	1.16	0.37	396266	2948	177	92	108
142	31BU-2	H17	3885	8960	4966	Crinoid (NL)	4.69	-2.47	11.21	0.17	0.30	0.14	0.015	11.38	2.19	0.44	396635	2697	146	75	166
143	31BU-4	H17	3885	8960	4966	Crinoid (NL)	4.39	-3.08	15.31	0.21	0.21	0.15	0.014	15.52	1.42	0.35	395257	3670	185	79	114
144	31BU-5L	H17	3885	8960	4966	Crinoid (NL)	4.48	-2.86	12.00	0.21	0.21	0.18	0.018	12.21	1.14	0.39	396350	2885	182	99	115
145	31BU-5R	H17	3885	8960	4966	Crinoid (NL)	4.58	-2.81	15.56	0.24	0.39	0.17	0.015	15.79	2.28	0.56	395163	3728	204	93	214
146	31BU-7	H17	3885	8960	4966	Crinoid (NL)	4.50	-2.87	12.76	0.22	0.44	0.17	0.017	12.99	2.65	0.61	396091	3066	193	90	243
147	031-2	F08	3818	9090	5408	Crinoid, Tiger	4.93	-2.16	9.38	0.18	0.36	0.08	0.019	9.56	4.68	0.44	397234	2260	158	42	201
148	031-3	F08	3818	9090	5408	Crinoid, Tiger	4.92	-2.01	9.37	0.18	1.71	0.06	0.019	9.55	26.88	1.77	397239	2257	157	35	944
149	071-3L	F13	3833	9137	5416	Crinoid, Tiger	4.20	-4.80	45.11	0.28	2.12	0.19	0.006	45.39	11.40	2.31	385665	10550	235	98	1139
150	071-3R	F13	3833	9137	5416	Crinoid, Tiger	4.07	-5.12	40.52	0.29	2.85	0.23	0.007	40.82	12.64	3.07	387096	9513	250	120	1535
151	091-1C1	F15	3981	9165	5312	Crinoid, Tiger	5.13	-2.65	9.22	0.15	0.43	0.11	0.016	9.37	3.91	0.53	397308	2222	127	59	236
152	091-1C2	F15	3981	9165	5312	Crinoid, Tiger	5.14	-2.31	10.84	0.18	0.30	0.01	0.016	11.02	3.11	0.40	396754	2608	153	53	168
153	091-3L	F15	3981	9165	5312	Crinoid, Tiger	5.18	-1.86	10.00	0.15	0.38	0.09	0.015	10.15	4.13	0.47	397048	2407	132	50	208
154	091-3U	F15	3981	9165	5312	Crinoid, Tiger	5.15	-1.76	10.27	0.16	0.37	0.10	0.016	10.43	3.69	0.48	396953	2471	140	55	207

Row	Sample	Site	EAST	NORTH	ELEV	Category	$\delta^{13}C$	$\delta^{18}O$	Mg/Ca	Sr/Ca	Fe/Ca	Mn/Ca	Sr/Mg	Mg+Sr	Fe/Mn	Fe+Mn	Ca	Mg	Sr	Mn	Fe
							(‰ VPDB)		(mmol/mol)								(ppm)				
155	092-3C	F15	3981	9165	5312	Crinoid, Tiger	5.20	-1.95	9.29	0.16	0.21	0.07	0.017	9.45	2.79	0.28	397279	2239	136	40	114
156	17AU-1	H03	3751	9129	5448	Crinoid, Tiger	4.72	-4.64	29.85	0.20	1.04	0.12	0.007	30.05	8.94	1.16	390543	7069	173	62	567
157	17AU-2	H03	3751	9129	5448	Crinoid, Tiger	4.74	-5.46	26.60	0.22	0.80	0.10	0.008	26.82	7.70	0.91	391580	6317	185	56	438
158	17AU-3	H03	3751	9129	5448	Crinoid, Tiger	4.46	-6.40	31.99	0.28	1.03	0.13	0.009	32.27	7.91	1.16	389813	7562	240	70	560
159	17AU-4	H03	3751	9129	5448	Crinoid, Tiger	4.74	-4.91	27.22	0.24	1.24	0.10	0.009	27.46	11.83	1.34	391368	6460	204	56	676
160	17B-1	H03	3751	9129	5448	Crinoid, Tiger	4.88	-5.86	29.18	0.25	1.02	0.12	0.008	29.42	8.84	1.13	390733	6914	210	62	553
161	17B-2	H03	3751	9129	5448	Crinoid, Tiger	4.79	-5.65	39.28	0.16	1.45	0.10	0.004	39.45	14.18	1.56	387560	9233	139	55	785
162	17B-3	H03	3751	9129	5448	Crinoid, Tiger	4.81	-3.20	29.54	0.24	1.40	0.12	0.008	29.78	11.47	1.52	390621	6997	205	65	761
163	17B-4	H03	3751	9129	5448	Crinoid, Tiger	4.79	-4.81	50.57	0.19	1.47	0.09	0.004	50.76	16.28	1.56	384010	11776	163	47	785
164	18U-3	H04	3735	9133	5401	Crinoid, Tiger	4.58	-3.48	18.61	0.21	0.52	0.14	0.011	18.82	3.71	0.66	394176	4448	184	76	288
165	18U-5	H04	3735	9133	5401	Crinoid, Tiger	4.56	-3.53	10.67	0.22	0.76	0.16	0.021	10.89	4.71	0.92	396785	2567	191	87	417
166	19-1	H05	3734	9122	5359	Crinoid, Tiger	4.55	-3.60	8.78	0.21	0.45	0.13	0.024	8.99	3.49	0.58	397419	2116	182	70	248
167	8A1-1	F14	3906	9190	5410	Crinoid, Tiger	4.43	-2.19	7.68	0.16	1.01	0.34	0.021	7.84	2.98	1.35	397811	1853	142	185	560
168	8A1-2	F15	3981	9165	5312	Crinoid, Tiger	4.76	-2.25	-	-	-	-	-	-	-	-	-	-	-	-	-
169	8A1-3	F16	4016	9075	5180	Crinoid, Tiger	4.50	-2.22	-	-	-	-	-	-	-	-	-	-	-	-	-
170	8A1-5	F17	4081	9053	5139	Crinoid, Tiger	4.77	-1.82	7.85	0.14	0.36	0.13	0.018	7.99	2.82	0.48	397767	1893	124	69	198
171	301-2	H16	3914	9002	5043	Crinoid (VL)	4.56	-2.22	13.25	0.22	0.29	0.30	0.016	13.47	0.96	0.58	395933	3182	188	161	158
172	322-1	H18	3852	8934	4945	Crinoid (VL)	4.83	-1.83	13.90	0.20	0.21	0.06	0.015	14.11	3.25	0.27	395727	3336	176	34	113
173	322-2	H18	3852	8934	4945	Crinoid (VL)	4.89	-2.14	9.90	0.17	0.23	0.09	0.017	10.07	2.46	0.32	397070	2383	147	50	125
174	322-3	H18	3852	8934	4945	Crinoid (VL)	4.82	-3.19	10.26	0.15	0.25	0.01	0.015	10.42	2.61	0.34	396958	2471	133	52	138
175	092-1L	F15	3981	9165	5312	Crinoid (VL)	5.14	-1.87	8.80	0.14	0.25	0.14	0.016	8.94	1.81	0.39	397451	2122	122	76	139
176	31BU-6	H17	3885	8960	4966	Crinoid (VL)	4.45	-1.88	10.54	0.17	0.13	0.33	0.016	10.72	0.41	0.46	396854	2538	151	177	73
177	031-1	F08	3818	9090	5408	Brachiopod (NL)	3.47	-2.85	4.22	0.83	2.63	0.27	0.197	5.06	9.76	2.90	398573	1021	726	147	1461

*L = Luminescent, NL = non-luminescent, VL = variably luminescent, C = cave, S = syntaxial, B = Bulk
**East = UTM Easting, add 041 to beginning, North = UTM Northing add 362 to beginning, Zone = 13S

Category	*n*	$\delta^{18}O$				$\delta^{13}C$				Mg/Ca				Sr/Ca				Fe/Ca				Mn/Ca			
		Min	**Max**	**Avg**	**SD**	**Min**	**Max**	**Avg**	**SD**	**Min**	**Max**	**Avg**	**SD**	**Min**	**Max**	**Avg**	**SD**	**Min**	**Max**	**Avg**	**SD**	**Min**	**Max**	**Avg**	**SD**
Micrite	17	-7.0	-1.6	-3.8	1.5	0.3	5.0	4.0	1.2	6.71	102.2	20.03	28.2	0.37	1.36	0.72	0.23	0.27	49.94	4.67	11.81	0.14	7.70	1.08	1.81
Cement, Cave	5	-3.7	-3.0	-3.23	0.3	-9.4	-8.1	-8.6	0.6	0.60	1.16	0.72	0.3	0.01	0.02	0.00	0.01	-0.06	1.56	0.44	0.64	0.01	0.23	0.08	0.09
Cement, Syntaxial	5	-8.1	-0.6	-2.88	3.5	3.8	5.1	4.6	0.6	3.61	11.07	6.61	2.8	0.12	0.23	0.15	0.05	0.50	3.07	1.76	1.03	0.08	0.91	0.37	0.34
Cement, Non Lum	35	-6.0	-1.3	-4.04	1.5	2.3	5.1	4.5	0.6	8.17	21.58	11.76	3.0	0.14	0.36	0.21	0.05	0.01	7.67	1.19	1.55	0.08	0.46	0.15	0.07
Cement, Lum	5	-6.7	-2.8	-4.58	1.4	3.0	4.4	3.9	0.5	7.34	20.32	11.38	6.1	0.15	0.33	0.22	0.08	0.18	1.50	0.86	0.65	0.22	2.23	0.78	0.97
Crinoid, Bulk	23	-5.2	-1.3	-2.58	0.8	3.8	5.2	4.6	0.4	6.17	44.09	12.82	11.5	0.28	1.54	0.66	0.33	0.28	2.96	1.08	0.86	0.04	0.84	0.26	0.20
Crinoid, Non Lum	34	-5.0	-1.6	-2.95	0.9	3.1	5.2	4.3	0.4	5.85	40.53	13.84	7.3	0.10	0.39	0.21	0.06	0.17	4.61	0.58	0.80	0.04	0.90	0.19	0.15
Crinoid, Lum	18	-4.6	-1.7	-3.14	0.8	-1.2	4.9	3.7	1.6	5.45	25.15	13.19	5.4	0.16	0.32	0.23	0.06	0.25	54.43	3.73	13.07	0.19	13.12	2.26	3.21
Crinoid, Tiger Lum	24	-6.4	-1.8	-3.53	1.5	4.1	5.2	4.8	0.3	7.68	50.57	21.45	13.9	0.14	0.29	0.20	0.05	0.21	2.85	0.97	0.67	0.06	0.34	0.13	0.06
Crinoid, Patchy Lum	6	-3.2	-1.8	-2.19	0.5	4.5	5.1	4.8	0.3	8.80	13.90	11.11	2.0	0.14	0.22	0.18	0.03	0.13	0.29	0.23	0.05	0.06	0.33	0.17	0.11
Bryozoan, Non Lum	2	-4.2	-2.7	-3.43	1.0	3.3	3.6	3.5	0.2	5.74	6.62	6.18	0.6	0.12	0.13	0.12	0.00	0.22	0.57	0.39	0.25	0.34	0.43	0.38	0.07
Bryozoan, Lum	2	-5.4	-4.2	-4.78	0.8	3.5	3.9	3.7	0.3	4.87	9.02	6.95	2.9	0.18	0.18	0.18	0.00	0.73	2.03	1.38	0.92	0.41	0.48	0.44	0.05
Brachiopod, Non Lum	1	-2.9	-2.9	-2.9	-2.9	3.5	3.5	3.5	3.5	4.22	4.22	4.22	4.2	0.83	0.83	0.83	0.83	2.63	2.63	2.63	2.63	0.27	0.27	0.27	0.27

Appendix 2: Summary statistics (Maximum, minimum, average, and standard deviation) for sample categories.

Reference	**Material**	$\delta^{18}O$	$\delta^{13}C$
Meyers and Lohmann, 1985	Carbonate cements, New Mexico	-1.5	4.3
Lohmann and Walker, 1989	Carbonate cements	-1	4
Douthit, 1990	Carbonate cements, Ireland	-1.9	4
Frank and Lohmann, 1996	Carbonate cements, New Mexico	-0.5	3.8
Veizer et al, 1999	Brachiopods, Global dataset	-4	2.5

Appendix 3. Estimates of Early Mississippian marine calcite compositions.